UNIVERSITÀ DEGLI STUDI DI MILANO

SCUOLA DI DOTTORATO IN SCIENZE MORFOLOGICHE, FISIOLOGICHE E DELLO SPORT

DOTTORATO DI RICERCA IN FISIOLOGIA

Dipartimento di Fisiopatologia medico chirurgica e dei trapianti

CICLO XXVII°

**Tesi di Dottorato di Ricerca**

# Recumbent vs Upright Bicycles: operative range of propulsive muscles, 3D trajectory of Body Centre of Mass and limb mechanical work

**Dottorando:** Riccardo Telli

Matricola: R09663

**Tutor:**          Prof. Alberto E. Minetti

**Coordinatore:**   Prof. Michele Mazzanti

**Anno Accademico 2013-2014**

**Tesi autorizzata dal coordinatore**

**Prof. Michele Mazzanti**

UNIVERSITÀ DEGLI STUDI DI MILANO

DOCTORAL SCHOOL IN PHYSIOLOGICAL, MORPHOLOGICAL AND SPORTS SCIENCES

## PhD Program in Physiology

Cycle XXVII°

**PhD Thesis**

# Recumbent vs Upright Bicycles: operative range of propulsive muscles, 3D trajectory of Body Centre of Mass and limb mechanical work

**PhD student:** Riccardo Telli

Matricola: R09663

**Tutor:**        Prof. Alberto E. Minetti

**Coordinator:**    Prof. Michele Mazzanti

# Index

## CHAPTER  3: RESULTS

## CHAPTER  4: DISCUSSION

## CHAPTER  5: CONCLUSION

## References

# Summary

**Introduction.** Humans have always tried to move safely and faster in a variety of environment, even through the aid of passive tools that help to improve the limits imposed by the body characteristics. These means of locomotion, without supplying additional mechanical energy, are able to greatly improve the performance exploiting the use of muscular force alone. Bicycles are probably the passive tool most known and used in the world. The origin of this thesis comes from the interest to increase the knowledge about the features of a particular kind of bike: the Recumbent bicycle (RB). It is a high performance human powered vehicle where the cyclist is in a reclined position, with the back against a backrest. The peculiarity of the RB is that it allows to reach higher speeds than Normal/upright bicycles (NB), at the same metabolic power, principally due to aerodynamic advantages. Indeed, with the use of particular fairings that improve aerodynamics, these vehicles allow to exceed 130 km/h only with muscles power. The change in posture of the rider, consequent to the different characteristics and design of the bicycles, alters kinematics and energetics of cycling and could also affects muscle-tendon lengths and the operating range of the muscles length-tension curves. Despite the interest of the scientific community on the topic of cycling, some aspects still need to be investigated, especially with respect to the differences between traditional and recumbent bikes, which represent the most advanced evolution of that tool.

**Aim.** The aim of this work is to analyze and compare the pedalling cycle on both bicycles from a biomechanical point of view. Indeed, with a comprehensive description of mechanical and metabolic consequences during cycling in both configuration, new vehicles could be designed with those technological changes that could increase the performance. Particular focus has been posed on the effect of the different position while riding the two bicycles:

- on the muscle-tendon length of different muscle-tendon unit involved in cycling;

- on the 3D displacement of the Body Centre of Mass (BCoM);

- on the mechanical work (in particular the internal and the "additional" external mechanical work).

**Methods.** The issues have been investigated both experimentally and trough simulations. By using 3D kinematic data and a physical simulation program we measured muscles-tendon length, 3D Body Centre of Mass (BCoM) trajectory and its symmetries and the components of the total mechanical work necessary to sustain cycling during stationary cycling, at different pedalling cadences (50, 70, 90 and 110 rpm). This approach allows to investigate the biomechanics of riding the two bicycles both through direct measurements of mechanical work and indirect estimation performed with simulation models.

**Results and Discussion.** Joint kinematics and muscle-tendon length were analyzed with the musculoskeletal modelling software Opensim®. This analysis showed that, differently from cadence, the two bicycles caused changes in joint angles and, consequently, in muscle-tendon length. As a results in RB, when compared to NB, some muscles are slightly stretched while other are shortened, making the propulsive effectiveness impossible to be assessed. This work confirms experimentally, for the first time, that the BCoM in cycling moves along all three spatial axes, while before this study an elliptical movement in the sagittal plane was appreciated only with a 2D simulation. BCoM trajectory, confined in a 15 mm side cube, changed its orientation maintaining a similar pattern in both configurations, with advantages for RB: a smaller additional mechanical external power (on average 16.1 ± 9.7 W on RB versus 20.3 ± 8.8 W on NB), a greater Symmetry Index on progression axis and no differences in the internal mechanical power (ranged from 7.90 W to 65.15 W in NB and from 7.25 W to 62.16 W in RB, increasing as function of the rpm).

**Conclusion.** Despite the human physiological characteristics have remained almost unchanged over the last millennia, performance on bicycles has increased significantly. This has been possible thanks to the work of mechanical engineers, exercise physiologists and biomechanists. In this thesis the body centre of mass trajectory and the associated additional external mechanical work while pedalling on recumbent bicycle has been studied experimentally for the first time. It is thought that the development of mechanisms reducing additional external power through a further containment of BCoM trajectory, together with additional studies on the effectiveness of propulsive muscles could be necessary to further refine design and improve performance of RB.

# Prologue

Humans have looked for ways to increase movement performance since civilization has existed and, more generally, they always aspire to save energy also when moving fast in order to keep low the energy cost of transport. During my doctoral studies in human physiology I focalized my research interest in the field of biomechanics of human locomotion and in this part of the thesis I want to briefly describe the work done in the last three years.

My main project titled "Recumbent vs Upright Bicycles: operative range of propulsive muscles, 3D trajectory of Body Centre of Mass and limb mechanical work " is submitted on a peer reviewed journal. **Chapter one** is a general introduction to recumbent bicycles and a review of the literature with a general presentation of the main biomechanical variables analysed. **Chapter two** represents the explanation of the methods utilized during the experiments. Subjects characteristic, protocol, instrumentation together with modelling software utilized be presented in this section. **Chapter three** shows all the results obtained from both experimental trials and simulations. **Chapter four** explains the data previously reported in the two pedalling position and, where possible, compares the experimental results with the data that came from the simulations. This thesis ends with the **Chapter five** where final conclusions, limits and future developments for the work are presented.

In this study we investigated the mechanisms involved in two different pedalling positions, recumbent versus upright, with the aim to provide hints and suggestions to evaluate the determinants of the performance, and to refine bicycles in the perspective of design a standard model that, for recumbent, has not been found yet. Besides experimental kinematic analysis, physical simulation of pedalling cyclist and musculoskeletal modelling were exploited here to describe the non-aerodynamic components that affect the total mechanical work, the effects on the displacement of the body centre of mass and its symmetries, and the range of contraction of different muscle tendon units.

Another part of my PhD period was spent to study the coordination between breathing rhythm and leg movements during running. While quadrupeds generally synchronize locomotor and respiratory cycles due to mechanical constraints, humans do not always show an alignment of the two frequencies. The aim of that work was to evaluate the locomotor-respiratory coupling during downhill running, with the hypothesis that the increased impact

load of the foot with the ground due to the speed and gradient could affects the breathing rhythm, forcing the start of the expiratory cycle in a specific point of the step cycle.

These two projects are not linked together, for this reason I decided to focus my thesis on the first study which involved many aspects of biomechanics of human locomotion. Moreover, it allowed me to learn experimental techniques for modelling the human body and simulate its interaction and movement with the environment.

# CHAPTER ONE

# Recumbent vs Upright bicycles: a literature review

## 1.1 Introduction

Over the course of history, the need to get food, capture prey , escape in case of danger and adapt to climate changes forced humans to move faster and economically in all terrestrial environments. Generally, animals use different means of locomotion in accordance with the habitat in which they live: birds use wings, fish exploit the fins to maximize propulsion in the water while terrestrial mammals move using limbs. We can speculate that many animals evolved reaching an anatomical structure and a pattern of movement that increase maximum speed, allowing them to catch more prey or to escape from predators (Alexander, Principles of animal locomotion), but it is not true for all species. However, maximum speed of movement is only used in case of need, because the top speed cannot be maintained for a prolonged time. Moreover, some animals (and also humans) can adapt their gait to the environment by challenging the combination of different locomotion modes while other have specialized their motion. Human locomotion is characterized principally by walking and running and, in some cases and particular condition, by skipping (a particular gait appreciable mostly in children). In many kind of locomotion is appreciable a typical pattern, defined by a rhythmic displacement of the body segment necessary to maintains the forward progression. In addition, the intelligence of which humans are equipped with allowed them to improve their speed of progression and their power even through the aid of passive tools. Humans developed a lot of means of transport trough the history but in thesis we will analyze only bicycles, a human powered vehicle that do not add extra mechanical energy to that generated by our own muscles. Indeed, as with skis (Formenti et al. 2005; Formenti & Minetti 2007), wheelchairs (Ardigo` et al. 2005) and halteres (Minetti & Ardigò 2002) the evolution of the bicycles is an example of one of the external devices that improved locomotion capabilities and compensate to certain limitations imposed by the human machine.

Since its introduction, the invention of bicycle reduced the required metabolic energy necessary to sustain locomotion in different ways:

_ by minimizing the vertical excursion of the body's centre of mass, most of which is supported by the saddle and not by the limbs, allowing muscle power to be exploited mainly for propulsion rather than for posture maintenance;

_ by reducing the speed oscillations because of the wheels;

_ by allowing muscles to operate in an efficient range of the contraction velocity, because of gears, despite of the high progression speed (di Prampero 2000; Minetti et al. 2001).

Since the Hobby Horse (figure 1) were introduced in 1820s, bicycles consented to move the lower limbs more slowly compared to the progression speed, differently from walking and running where the foot needs to be repositioned on the ground during each step (Saibene & Minetti, 2003). This bicycle consisted in two wooden wheels connected by a wooden beam on which a saddle, arm and chest support and a handlebar were fixed.



**Figure 1.** A typical example of Hobby Horse Bicycle.

This means of locomotion, differently from walking and running, supported some of the subject's weight allowing to save energy. Also other advantages occurred during the twentieth century. Indeed, in order to increase progression speed the pedals were introduced and the rotary movement also contributed to reduce the mechanical work. Muscles efficiency was optimized by using gears while rolling resistance and aerodynamic drag were reduced with the use of inflated tyres, lower mass and the design of new vehicles (Minetti et al. 2001) which also include the Recumbent Bicycle (RB).

## 1.2 History of Recumbent Bicycle

Recumbent Bicycle is known as that vehicle where the rider is in a laid-back reclined position. The comfort advantages over Normal/upright Bicycle (NB) can be summarized in a less saddle soreness, neck strain could reduced and visibility increased due to the natural forward position of the head that could be further helped by a headrest. It is also assumed that the head is in a more protected situation compared to NB if a crash occurs (Wilson et al., 1984). Despite the common opinion that it is a recent invention, it was introduced in the late 1800s and maintained a reputation as a bicycle built for comfort instead of speed until the 1930s, when French inventor Charles Mochet's version began to win races and claim speed records against traditional upright bicycles. Indeed, his further supine bicycle named "velocar" allows reaching higher speed at the same metabolic power compared to the NB principally due to aerodynamic advantages (Gross, Kyle & Malewicki, 1984). Thus, on 1933, Francis Faure, while riding the Velocar (Figure 2), broke the 20 year-old hour record of 44.247 km by going 45.055 km.
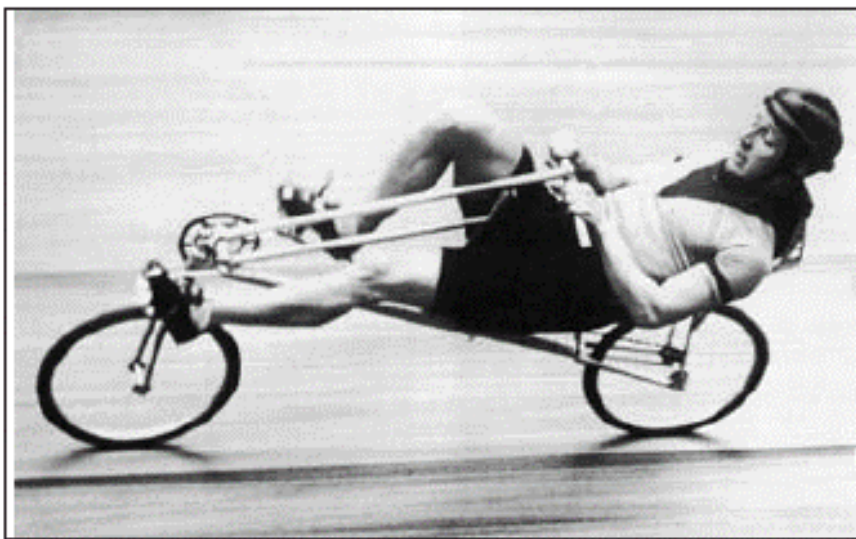


**Figure 2.** The French bicycle racer Francis Faure riding a Mochet "Velocar" recumbent during a 1933 speed record attempt.

Unfortunately, the record of Faure's created a dispute amongst the Union Cycliste Internationale (U.C.I.), the governing body for bicycle races. In February 1934, the U.C.I. decided not to validate his record and banned all recumbents and aerodynamic devices from official competitions. After the decision if the UCI, the International Human Powered Vehicle

Association (IHPVA) was founded. The IHPVA serves as the sanctioning body for new World Records in human powered land, water and air vehicles established in accordance with the Rules of the IHPVA. It can also act as a sanctioning body for races and other sporting events and records in non-stored-fuel land, water and air vehicles. To further these goals, the IHPVA organizes and promotes periodic competitions on land, water and in the air. Each year, the IHPVA holds or sanctions a human powered speed championships. The principal goal of this sporting event is to combine the best in technology and in athletic performance to get the fastest and most efficient human powered in different environmental conditions. Moreover it is an important moment to showcase ongoing technological development for speed and for practical human powered vehicles. The philosophy and policy of the association is to stimulate and promote competition and creativity. In order to promote competition and creativity, only few and simple restrictions have been created on bicycles design. For this reason there is not a single model of RB: this HPV is typically foot-powered, but some models use hand-crank in addition to foot pedals. The steering can be positioned above or under the seat, with the radius of the wheels that vary from model to model, with the front wheel that is generally smaller than the rear.

Despite the UCI decision and that the best model still remains to be designed, the quest for the maximal human speed on land received further impulse with these vehicles and the currents records on faired RB (reported in Table 1) exceed 130 km/h for men and 110 km/h for women riders, while the top speeds in a full faired NB is just below 83 km/h.

| Rider | Location | Date | Competition | Speed (km/h) |
|---|---|---|---|---|
| Sebastian Bowier | Battle Mountain, NV | 09/14/2013 | 200 m flying start speed trial, Men | 133.78 (top speed) |
| Barbara Buatois | Battle Mountain, NV | 09/15/2010 | 200 m flying start speed trial - Women | 121.81 (top speed) |
| Sam Whittingham | Romeo, MI | 07/19/2009 | 1 hour record standing start, Men | 90.60 (average speed) |
| Barbara Buatois | Romeo, MI | 04/07/2007 | 1 hour record standing start, Women | 69.63 (average speed) |

**Table 1.** Currents world speed record on full faired recumbent bicycles on two different categories.

# 1.3 Muscle properties

Human locomotion is allowed by striated muscles, which can be considered the muscles that powers locomotion. They are actuators generating force which can respond with positive or negative work, characterized respectively by concentric or eccentric contraction (Hull & Awkins, 1990). A contraction is done when the muscle generate force, but it can be concentric (the muscle shortens while under contraction), eccentric (when it lengthens) or isometric (when it generate force without changing length).

The functional unit of the fibre is the sarcomere, principally formed by protein filaments, built up from myosin thick myofibril and actin thin myofibril. The force-length relationship of sarcomeres may be explained, to a large degree, by the sliding filament and the cross-bridge theories. The first assumes that length changes in sarcomeres, fibres and muscles are accomplished by relative sliding of myofilaments. The cross-bridge theory suggests that the myosin head has enzymatic properties that allows to hydrolyze ATP into ADP, permitting a conformational change allowing the cross bridges to interact with the thin filament of actin and pull toward the midpoint of the thick filament. Each cross bridge attach, pull, detach with "an action like people pulling in a rope hand over hand" (Alexander Principles of animal locomotion). This allows the generation of force. The product of phosphorilation and contraction efficiency (respectively 0.6 and 0.5), is named muscle efficiency and can be at most 0.3.

Due to the fact that cross bridges have a limited attachment range, the attachments only occur in the actin-myosin overlap zone of a sarcomere (Figure 3).
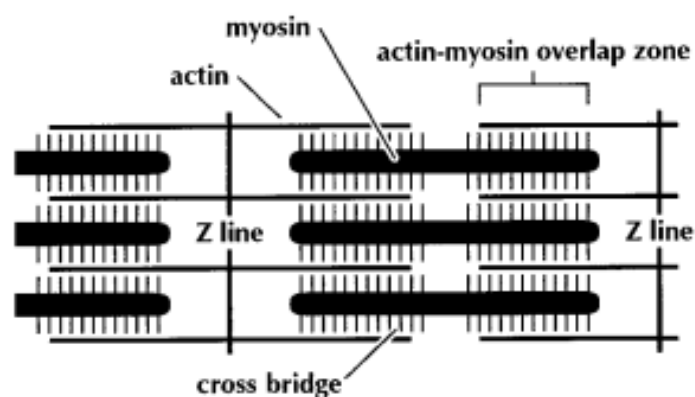


**Figure 3.** Schematic representation of a sarcomere.

The ability to generate force depends on the length of both the sarcomere and the muscle, and is maximum at intermediate length. The active force generated by a maximally activated single fiber, is maximal when the filament overlap is optimized and is proportionally decreased when overlap is diminished Figure 4.
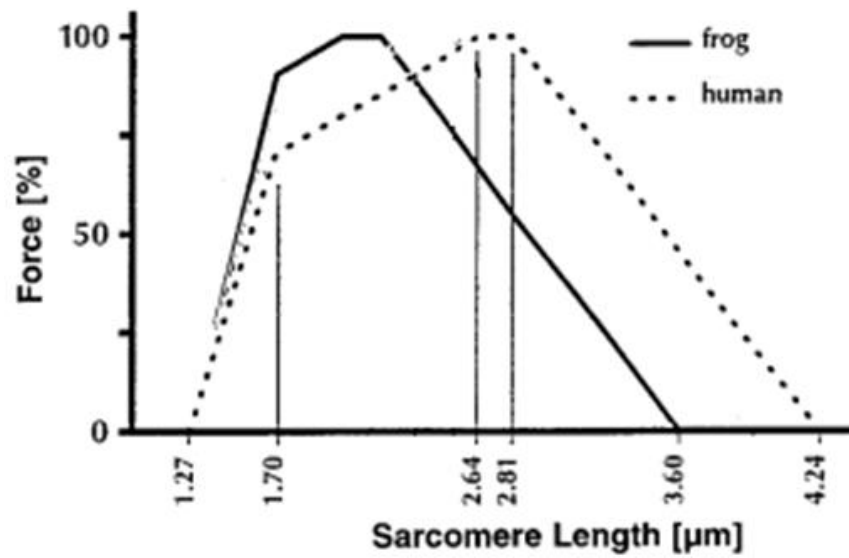


**Figure 4.** Force-length relationship of frog and human skeletal muscle sarcomere (Adapted from Raissier, 1999).

A similar relation can be shown analyzing the whole muscle even if attention must be paid to taking into account the bias resulting from the passive force contribution given by the muscular elastic components. However, the force/length characteristic of muscle does not penalize our daily activities because muscles are naturally built in order to operate along the optimal range. Movement is extremely important in animal kingdom, thus force is applied through a range of movement and velocity that gives origin to another important characteristic of the muscle contraction: the force-velocity relation. The ability to generate force depends also on the speed at which the muscle shortens: i.e. high contraction speeds are associated with low force production and vice versa (Hill, 1938).In sport competition, or when speed is a key element to any kind of performance, the capability to produce force over time, the power, is often more important than force and also a power-velocity relation can be established. Because the power is the product of force and velocity, at the extremes of the force-velocity curve the power generated is 0 while its highest value are placed at

about 1/3 of the maximum speed of the muscle. Also muscle efficiency, as well muscle force and power, depends on the velocity of contraction (Figure 5). Indeed, for a given temperature and fibre length, muscle force, power and efficiency are function of the ratio between *V* and *Vmax* (velocity of shortening and maximal velocity of shortening respectively).
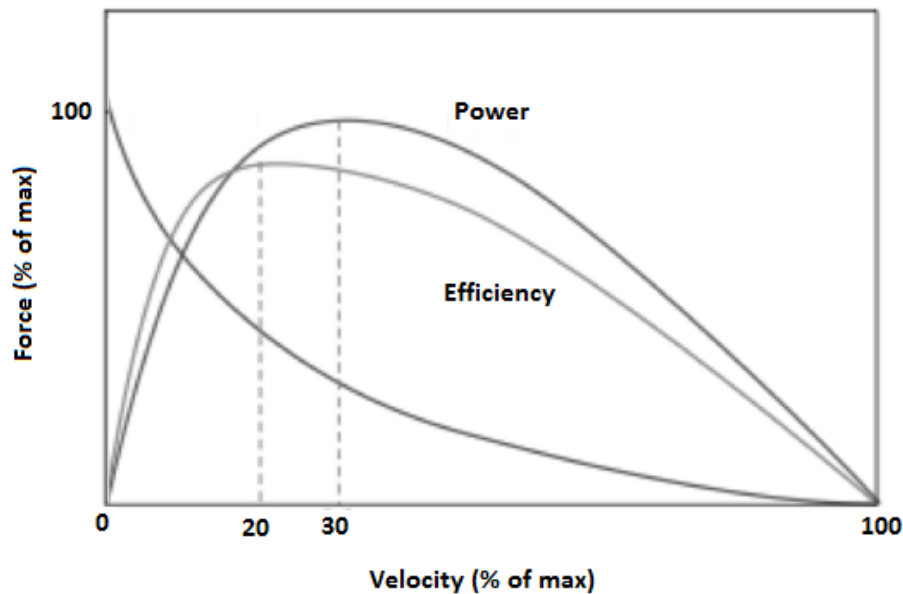


**Figure 5.** Muscle Force, Power and Efficiency as function of velocity of contraction. Both Force and Velocity are in percent of the maximum. Maximum efficiency is achieved at approximately 20% of the maximal shortening velocity (20 % of max), whereas maximal power is developed at approximately 30% of max. Adapted from Neptune et al., (2009).

Therefore, when muscles are closer or further to their optimal length, their ability to produce force is altered in accordance with the length-tension relationships (Rassier, 1999). Because alterations in cycling posture may elicit a favourable change in this relationship, allowing for greater force to be produced by a given muscle without additional energy expenditure, it is important to investigate how muscle length is altered when aspects of cycling are perturbed. The direct measure of the operating length of muscle tendon unit during locomotion is difficult to achieve, for this reason they will be estimated in this work with the OpenSim musculoskeletal modelling software.

## 1.4 Effect of Posture on Muscle Activity

In complex movement such in cycling, it is important to understand how the muscles were used to generate the forces needed to move the joints in order to generate and direct the power from the body to the pedal (Raasch & Zajac, 1999). The functional role of the muscles has been investigated in different ways like as EMG, force transducer and through computational modelling (Baum & Li, 2003; Brown et al., 1996; Neptune et al., 1997; Neptune et al., 2000; Raasch & Zajac, 1999; Raymond, 2005; Sanderson et al., 2006).

During 'downstroke' (from higher to lower position of the pedal), hip, knee and ankle joints extend to propel the bicycle, whilst in the recovery phase or 'upstroke' (from lower to higher position), they flex to pull the pedal back (Raymond 2005) (figure 6). Gregor and Conconi (2000) stated that during the recovery phase, the active flexion is useful to reduce the resistance and assist the contra-lateral limb in propulsion. In general, is well-accepted that uni-articulate muscles serve to generate energy for propulsion, while bi-articulate muscles serve to both transfer energy between segments as well as generate energy (Raymond 2005).
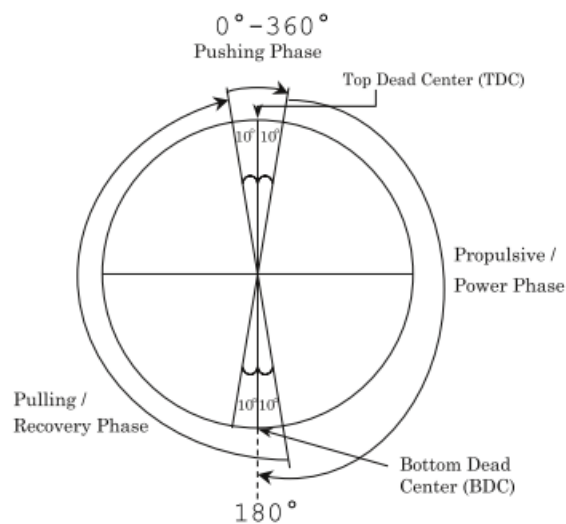


**Figure 6.** Schematic representation of de pedalling cycle (Adapted from Raymold et al., 2005)

It is reported that some muscles have a twice function depending on the phase of pedalling cycle: i.e. the rectus femoris assisted the hip flexion during the recovery phase, but in the propulsive one he is a knee extensor (Eisner et al., 1999). Hamstrings, that are considered knee flexors and have an important role in the recovery phase, are also active during the propulsive phase to extend the hip (Gregor et al., 1991).

The study of the muscles coordination in cycling in upright posture has received large attention, but it is not the same for recumbent position. Only one study of Hakansson and Hull (2005) has investigated the patterns of muscle activation over the crank cycle to compare the functional roles of muscles both in upright and recumbent posture. The authors reported that, when the crank cycle was adjusted for orientation in the gravity, the activation patterns for the two positions were similar.
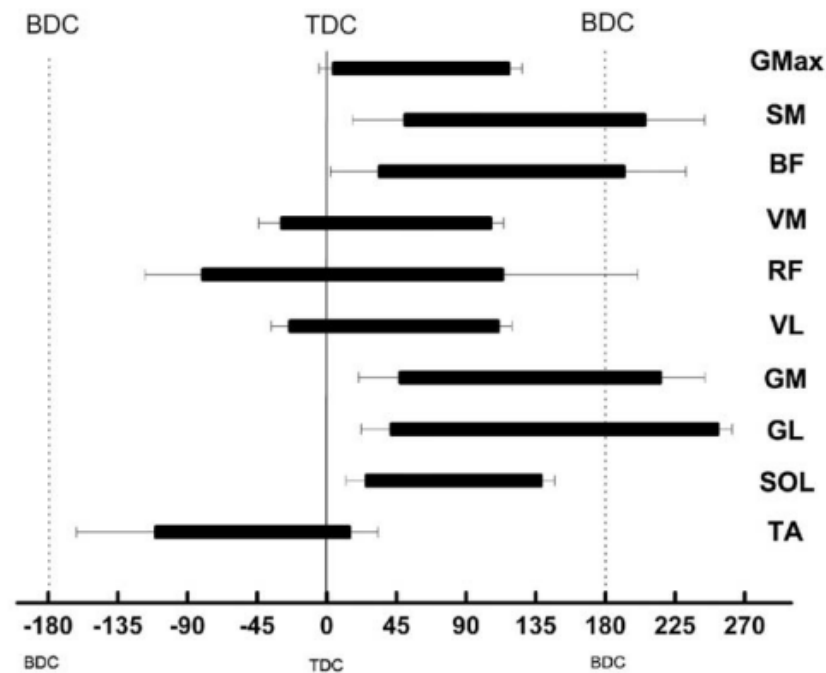


**Figure 7.** Mean onset, offset and duration of EMG activity phase indicated by horizontal bars for 10 lower limb muscles, displayed as function of crank position. TDC, top dead center (0°); BDC, bottom dead center (180°). GMax, Gluteus maximus; SM, Semimembranosus; BF, Biceps femoris (long head); VM, Vastus medialis; RF, Rectus femoris; VL, Vastus lateralis; GM, Gastrocnemius medialis; GL, Gastrocnemius lateralis; SOL, Soleus; TA, Tibialis anterior. Adapted from Dorel et al. 2007.

When muscles shorten more quickly or are closer or further to their optimal length, their ability to produce force is altered in accordance with the length-tension-velocity relationships (Rassier, 1999). Alterations in cycling posture and technique may elicit a favourable change in these relationships, allowing for greater force to be produced by a given muscle without additional energy expenditure. Therefore, it is important to investigate how muscle length is altered when aspects of cycling are perturbed. Because the direct measure of the operating length of muscle tendon unit during locomotion is difficult to achieve, they will be estimated with a musculoskeletal modelling software named OpenSim.

# 1.5 Effect of Posture on Performance

Engineers have principally been based on the bicycles characteristics while designing human powered vehicles. But when the minimal aerodynamic drag is reached, which will be the position of the riders on the bicycles? To further improve the speed of RB it is necessary to find the equilibrium between bicycle aerodynamics and the position of the riders that allows to optimize the performance of the human machine. Indeed, by changing the position of the subject on a bicycles alters both energetics and biomechanics of pedalling, and the effects of different posture in terms of seat tube angle, crank length and seat-to-pedal distance have been investigated both in upright (Faria et al., 2005) and recumbent cycling (Too, 1990). As reported by the authors, changes in these variables affect kinematics of cycling, joint angles and consequently muscle length and muscle moment arm length; therefore also the length-tension, force-velocity relationship and the efficiency of muscles could be altered. The characteristic of a bicycle and the position of the riders could affect the ability of cycle-rider system to generate power during pedalling cycle.

Upright standard position allows greater maximal power output and $VO_{2max}$ compared with aero or racing position (where the rider is in a crouched position using handlebars) (Ashe et al., 2003; Evangelisti et al., 1995) while in other two studies no differences were founded between standard and aero upright posture (Origenes et al., 1993; Hubenig et al., 2011). Furthermore the effect of different bicycles characteristics have been widely investigated in detail altering seat tube angle (Price & Donne, 1997 ; Silder et al., 2011; Heil et al., 1995; Bisi et al., 2012; Diaz et al., 1978), crank length (Inbar et al., 1983; Too & Landwer 2000; Martin & Spirduso 2001; Zamparo et al., 2002) and seat height (Price & Donne, 1997; Nordeen-Snyder, 1977; Shennum & Devries, 1976; Burke & Pruitt,2003; Gregor et al., 1991; Hamley & Thomas, 1967). Seat tube angle could alter biomechanical and metabolic responses in both aerobic and anaerobic condition in NB (Price & Donne, 1997; Silder et al 2011 ; Heil et al., 1995; Bisi et al., 2012) and in RB (Diaz et al., 1978), but results in literature are conflicting and the optimal seat tube angle remain still to be determined (Faria, 2005).

Regarding the effect of crank length, it was established that a crank length about 20% of the leg length or 41% of the tibia length is optimal for power production (Martin & Spirduso, 2001). More recently Zamparo et al found a lower VO2 consumption and a greater efficiency using a new pedal crank prototype, where the crank length changes as function of crank

angle increasing the torque exerted during pushing phase and decreasing the counter torque caused by the contra-lateral recovering phase. The difference between new and standard pedal crank was present only when the exercise intensities were between 250-300 W (Zamparo et al., 2002). The oxygen consumption in cycling is minimized with a seat to pedal distance (or seat height) of 100% of trochanteric leg length or at about 105% of symphysis pubic height (Burke & Pruitt, 2003) and a decreases in seat to pedal distance is accompanied to an increase in quadriceps and hamstring muscle groups activity (Gregor, et al., 1991). A value of 109% of symphysis pubis height is optimal for an anaerobic performance (Hamley & Thomas, 1967) while a 100% of the trochanteric leg length is recommended for aerobic performance (Nordeen-Snyder, 1977). Moreover is recently reported that modifications in bicycle setting could affect the racer position and motion during pedalling; also small changes in saddle height (2%) affect significantly lower leg kinematics and gross efficiency during sub-maximal pedalling (Ferrer-Roca et al., 2014).

Performance while cycling in recumbent posture is reduced only when the recumbent trunk rest angle is 15° or lower (Egana et al., 2010; Egana et al., 2013). Moreover, studies on the metabolic effects of different cycling positions stated that the upright posture allows the subjects to sustain exercise longer than the supine one (Terkelsen et al., 1999; Leyk et al., 1994; Egana et al., 2006) with advantages in terms of lactate production and oxygen uptake kinetics (Koga et al., 1999; Convertino et al., 1984; Hughson et al., 1991; Leyk et al., 1994). This is probably due to the fact that endurance and fatigue during exercise are sensitive to the vertical distance between the heart and the active muscles because of the gravitational effect acting across the involved muscles (Eiken, 1988; Egana & Green, 2005).

There are many factors affecting performance during human locomotion and some, like as metabolic expenditure, oxygen consumption, and lactate threshold, can be improved through physical training. But in modern cycling it is not enough to win a race or to reach speed record. As we have just seen, bicycles characteristics and biomechanical aspects should be also taken into account because cycling performance depends to various factors, each of which may play an important role.

# 1.6 Body Centre of Mass and Locomotion

The Body Centre of Mass (BCoM) is a physical imaginary point and can represents a relevant gait analysis variable. Indeed, by describing the BCoM it is possible to summarize the whole body movement and the translational vector for the momentum of the body mass. The three-dimensional (3D) trajectory of BCoM could represent a sort of 'locomotor signature' capable to reflect any significant change in the motion pattern and its description would summarise the general aspect of the gait and the individual characteristics of movement. In order to fully describe and quantify the individual behaviour of the BCoM during locomotion, a mathematical method has been recently proposed (Minetti et al., 2011), allowing to evaluate quantitatively its displacement and the dynamical symmetry between right and left steps along the three spatial axes.

Symmetry received much attention in the last two decades and played an important role in legged locomotion. This topic was introduced more than 80 years ago by Lund who showed the effects of structural/anatomical asymmetry on lateral drift in human locomotion. Body symmetry can be further modulated in sports: depending on the discipline, relevant muscles become asymmetrically different (tennis, fencing, throwing, etc.), or they are required to reach similar hypertrophy (ice-skating, downhill skiing, front crawl, etc.) on the two sides of the sagittal plane. Thus, body changes towards or from symmetry are not just the consequence of genetics and laterality, being also caused by specific training protocols. Several authors studied symmetry not only in human walking and running (Nardello et al. 2009; Seminati et al. 2013) but also in cycling (Smak et al., 1999). The analysis of the symmetry in cycling has been linked to the possibility to identify an optimal pedalling rate which more evenly distributes pedalling forces during pedalling cycle, with the hypothesis to reduce the risk of overuse injury (Smak et al., 1999). In this work the analysis of symmetry is related to the 3D trajectory of the body centre of mass. The analysis of the BCoM is also important to calculate the energies associated with it and to its relatives segments, allowing to investigate the mechanical work necessary to move.

# 1.7 Mechanical Work

Locomotion is the result of coordinated activity of muscles, that exerts force via tendons and allows to produce the movement of bones and, consequently, of body segments. More generally, all forms of locomotion are linked to the concept of mechanical energy required for contraction and relaxation of skeletal muscles and the associated mechanical and metabolic energy. The changes of mechanical energy over time (mechanical work) necessary to maintain body movement have been extensively studied since the first half of 1900 (Fenn 1930; Elftman 1939) and is needful for the analysis of the total mechanical work ($W_{tot}$) which has been classically divided (particularly in legged locomotion) into the mechanical external work to raise and accelerate the Body Centre of Mass within the environment, and the internal work defined as the work necessary to reciprocally accelerate body segments with respect to the BCoM (Cavagna et al., 1964, 1976; Cavagna & Kaneko 1977; Winter, 1979; Willems et al., 1995; Minetti and Saibene 1992; Minetti 1998) but it also include the work to overcome internal friction in body tissues (Fenn, 1930; Minetti, 2011). This approach is based on König's Theorem, which states that the total kinetic energy of a multisegment body is the sum of the kinetic energy of body centre of mass and the kinetic energy (translational and rotational) of all the segments relative to the BCoM (Saibene and Minetti 2003). The kinematical model has been adapted through the years in an attempt to accurately calculate the mechanical work during walking and running (Cavagna e Kaneko 1977; Winter 1979; Minetti et al., 1993; Willems et al.,1995).

In cycling, the external mechanical work ($W_{EXT}$) is referred to the work due to overcome rolling and air resistance and the metabolic energy spent against these components were studied by Di Prampero and collaborators (1979; Minetti et al., 2001). The mechanical external power ($\dot{W}_{EXT}$) in cycling represents the rate of energy applied to the pedal needed to win external forces (rolling and air) opposing to movement and is generally measured with commercial bicycle power meters (figure 8) such as PowerTap (CycleOps, WI, USA) and SRM Powermeter (Powermeter, SRM, Germany). In this work the external power will be considered only to check that the same power is reached, at the same pedalling frequency, in both bicycles.

**Figure 8.** Pictures show two instruments for the measure of the $\dot{W}_{EXT}$ in cycling, the SRM powermeter (a) and the PowerTap (b).

However, the common belief of the purely translational pattern of the BCoM in cycling was suggested not to be the case (Minetti, 2011). Rather, the small BCoM movements described an elliptical trajectory in the sagittal plane that could be responsible of a slight additional mechanical external work ($W_{EXT*}$) necessary to sustain the periodic lift and acceleration of the BCoM, even when pedalling seated on a saddle.

Particularly, mechanical external work in walking and running, proposed as $W_{EXT*}$ in cycling, accounts for the changes in potential (PE) and kinetic (KE) energies of the BCOM with respect to the environment (Minetti 2011). The mechanical external work can be divided into:

1. $W_{EXT*}^{+}$ : positive mechanical work necessary to raises and accelerates the BCOM (Minetti et al., 1993) and corresponding to an increase in total mechanical energy;

2. $W_{EXT*}^{-}$ : negative mechanical work needed to lowers and decelerates the BCOM and corresponding to a decrease in total mechanical energy (Minetti et al., 1993). Negative work in cycling is represented principally by aerodynamic drag and rolling resistance.

$W_{EXT*}$ can be obtained both using dynamometric platforms through direct dynamic, which is considered the gold standard, and cinematographic data through the inverse dynamics. In both cases, in order to study the "additional" external mechanical work, is necessary to start from the analysis of the BCoM. On this basis we decided to investigate the differences in the BCoM trajectories in the two cycling conditions with an experimental and theoretical approach. Studies regarding the metabolic equivalent of internal power ($\dot{W}_{INT}$) focused only on upright bicycles (Francescato et al., 1995; Tokui & Hirakoba, 2008). $\dot{W}_{INT}$ was modelled to

depend on the third power of the pedalling frequency (di Prampero, et al., 1979; Minetti et al., 2001). More recently Capelli et al. (2008) investigated the mechanical efficiency of RB, i.e. the ability to convert metabolic energy in mechanical work, by dividing the mechanical work per unit of distance and the corresponding cost of locomotion. They concluded that the change of position did not affect muscles efficiency.

# 1.8 Cost of Transport

As mentioned above, humans try to move faster and more economically during the course of history, even in sport competition. Velocity can be considered the critical measure to determinate performance in many sports and it is known that the maximal speed reached during locomotion depends primarily on the locomotion modes. Indeed, the world speed record achieved in 100 m frontal crawl is about 8 km/h, in running in near to 35 km/h, in normal cycling is more than 75 km/h while in full faired RB the velocity of 200 m speed trial can exceed 130 km/h. Because the maximal muscular power is similar in all athletes, the great difference of velocity is due to the locomotion type and to the metabolic energy spent per unit distance covered, a paramemeter introduced by Margaria (1938) and further called "cost of transport" (C) (Schmidt-Nielsen, 1972). C can be defined as the quotient of net metabolic power divided by speed of progression:

$$C \equiv \frac{\dot{V}O_2 - \dot{V}O_{2rest}}{s} * EQ$$

where $\dot{V}O_2$ is the oxygen consumption during exercise and $\dot{V}O_{2rest}$ the oxygen consumed at rest. The difference between $\dot{V}O_2$ and $\dot{V}O_{2rest}$ is the net metabolic power. EQ is the energetic equivalent related to the respiratory quotient and correspond to the energy burned per litre of oxygen consumed, s is the speed of progression.

It can be considered a parameter that characterises any type of locomotion because the velocity during locomotion is related to the rate of energy expenditure (or metabolic power) and C according to the following equation:

$$v \equiv \frac{E}{C}$$

where v is the velocity (m/s), E is the rate of total energy expenditure (J/s), and C is the metabolic cost of locomotion (J/m) (di Prampero, 1986). Applying maximal condition it results that, in speed independent locomotion:

$$v_{max} \equiv \frac{E_{max}}{C}$$

Because the $E_{max}$ is similar in all elite athletes in a specific discipline, this relation explain why the maximal speed attained ($v_{max}$) in the different locomotion modes is set by C.

In the specificity of our research area, enhancements in cycling performance could be attained both trough athlete training, that influence $E_{max}$, and by commercial product development, improving bicycles with a consequent reduction of C. It is well known that the C of bicycling (ranged from 0.3 to 4 J/kg/m depending on speed) is lower than walking (ranged from 1.5 to 4 J/kg/m depending on speed) and running (4 J/kg/m and speed independent) (Figure 9).
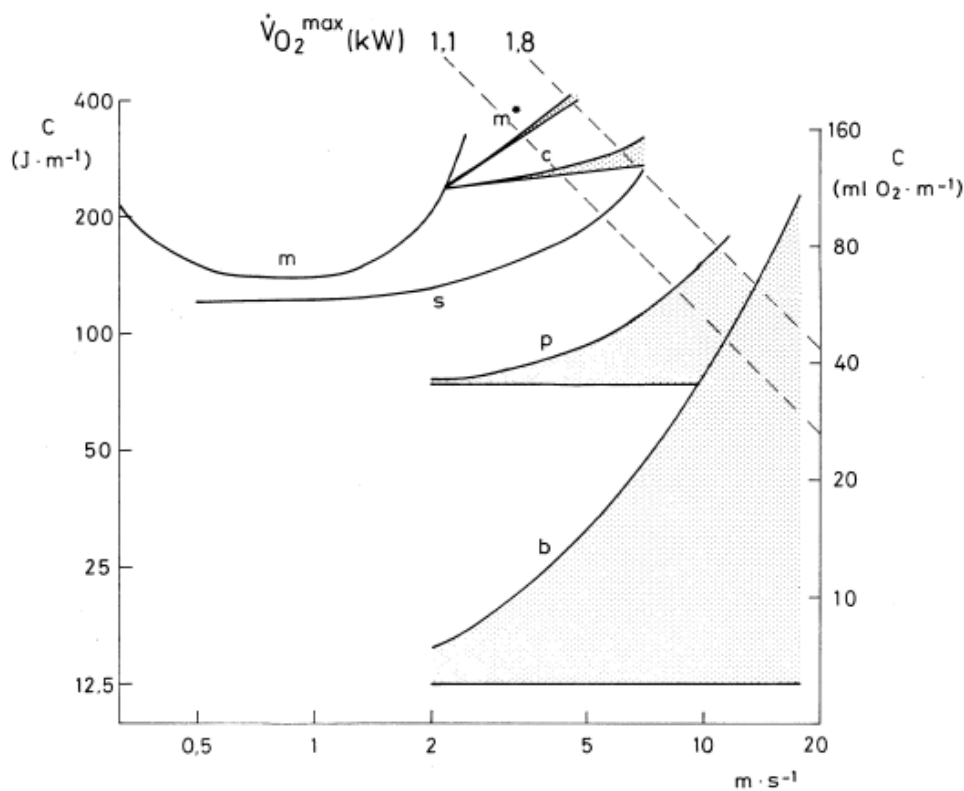


**Figure 9.** Metabolic cost versus progression speed of a typical subject of 70 kg and 175 cm height for different gaits: walking (m), race-walking (m*), running (c), cross-country skiing (s), ice skating (p) and cycling with racing bicycle in aerodynamic posture (b). Lower line represents non aerodynamic

energy cost, upper curves are the total cost of transport. (di Prampero, 1985. La locomozione umana su terra, in acqua, in aria. Edi Ermes - Milano 1985).

The increase of energy associated to the increasing speed during cycling is principally due to aerodynamic factor, as results from figure 9. Moreover, the evolution of the bicycles led to a progressive decrease of the metabolic cost during the history (Minetti et al., 2001) as shown in figure 10, where C is expressed in J/kg/m. Differently to running, cycling and skipping, C during walking shows a minimum at intermediate speed, generally the self selected speed, which is also called optimal walking speed. It is interesting to note that, similarly to walking, also C of the first invented bicycle (i.e. the Hobby Horse) can be empirically described by a quadratic equation: this is due to the fact that this kind of bike was not equipped with pedals.
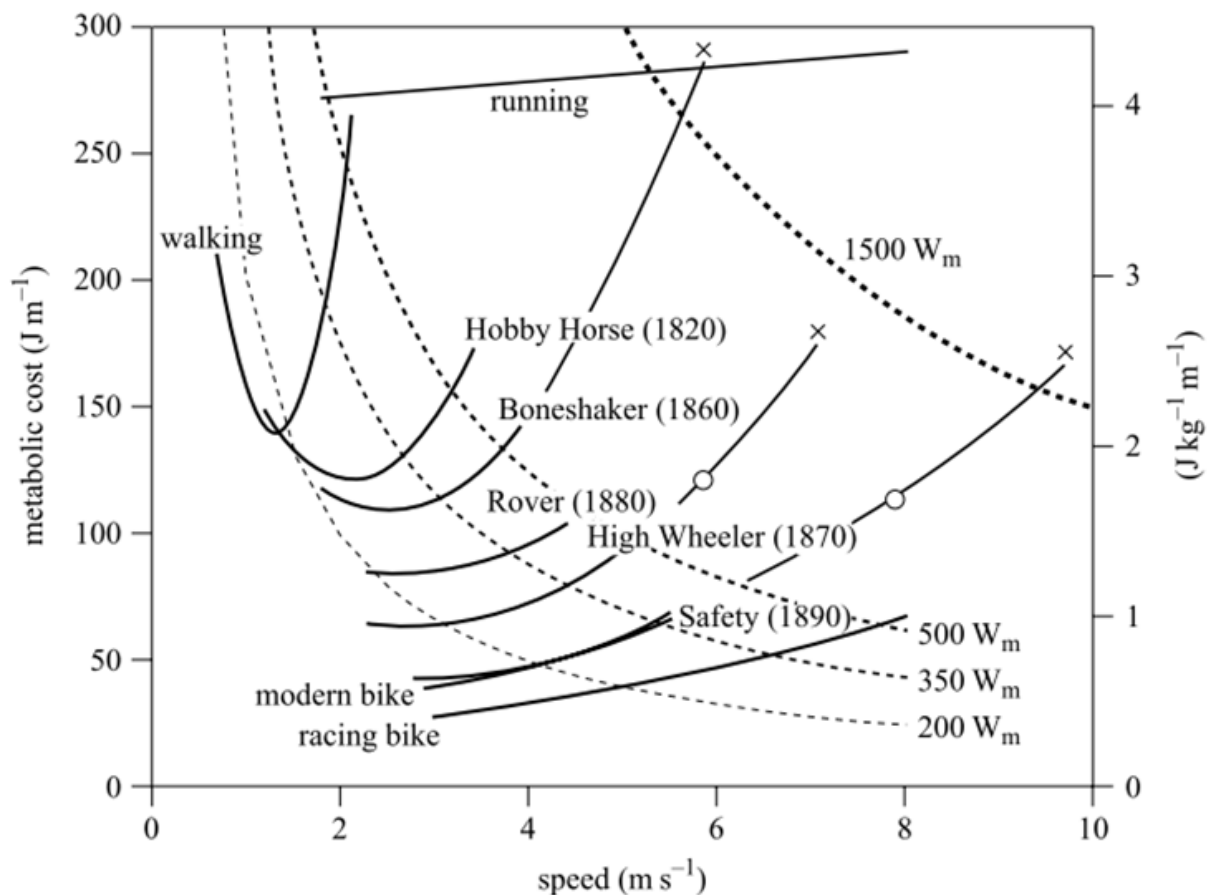


**Figure 10.** Metabolic cost of transport versus speed for different locomotion: walking, running and cycling different bicycle models. Dashed lines represent isometabolic power hyperbolas (power = cost X speed) (Wm represent metabolic watt) (Minetti et al., 2001).

In addition there is an optimal step frequency at each speed of progression, generally corresponding to the freely chosen, which minimize C both in walking (Zarrugh & Radeliffe, 1978; Zarrugh et al., 1974; Cavagna & Franzetti, 1986) and running (Hogberg, 1952; Kaneko et al., 1987; Morgan et al., 1994). It is well known that also in cycling there is an optimal pedal frequency, which increases with the mechanical power output, that minimizes C (di Prampero 1986).

Most researches on cycling focused principally on the metabolic aspects of performance, but the ability to increasing performances passes through the knowledge of the determinants of the energy expenditure of riding a bicycle. Di Prampero was the first investigator to divide the energy expenditure of cycling in the metabolic equivalent of the different forms of mechanical work done. He split the total external mechanical work into three components: the energy spent to overcome rolling resistance and other mechanisms of energy dissipation of the bicycle (Wev), the air drag (Wer) and the effect of inclined terrain (Weg). These aspects, together with the C of different modes of human locomotion, were investigated in depth (di Prampero, 1986).

# 1.9 Aim of the study

The purpose of this study is to investigate the mechanisms involved in the two different kind of pedalling. It is reasonable to assume that the change in posture of the rider affecting kinematics and energetics of cycling, could affect muscle-tendon lengths and the operating range of the muscles length-tension curves. For this reason we will compute also muscles-tendon length (MTL) in order to complete our analysis with the hypothesis that different cycling posture could be related to different behaviours of the human machine especially in term of performance. The 3D displacement of the Body Centre of Mass together with its associated energies will be calculated in order to successively evaluate the components of the total mechanical work necessary to sustain cycling, with the goal to highlight the differences between NB and RB at various cadence and corresponding external power ( $\dot{W}_{EXT}$ ). Internal power ($\dot{W}_{INT}$ ) will be considered as well as the additional external work rate ($\dot{W}_{EXT*}$) related to the BCoM displacement.

A whole evaluation of the determinants of the total mechanical work will provide hints and suggestions to refine RB in the perspective of design a standard model that, differently from NB, has not been reached.

# CHAPTER TWO

## Methods

### 2.1 Participants

Four healthy male subjects (age 28.25 ± 2.63 years; body height 1.77 ± 0.06 m; body mass 66.75 ± 4.11 kg) were recruited. All participants were not professional cyclists and they were free from any musculoskeletal injury. The institutional ethics committee of the University of Milan had approved all methods and procedures, and subjects, fully informed about the aim of the study, gave their written informed consent prior to the start of testing. Sample size has been chosen considering that this work consist on preliminary comparison between RB and NB and the range of variability of the analyzed parameters still remains to be determined. In addition cycling is a constrained stereotyped movement giving origin to a repeatable kinematics.

### 2.2 Experimental set-up and Protocol

After a period of familiarization with the rhythm imposed by a metronome, monitored also with the visual feedback given from the SRM Powermeter, subjects performed one minute of pedalling for each of the different cadences (50-70-90-110 rpm) in randomized order on NB and RB. In addition, subjects performed one minute of freewheel pedalling in order to measure the time course of pedal crank angular velocity at self-selected pedalling frequency. Bicycles were stationary placed on rollers and instrumented with an SRM powermeter (Powermeter, SRM®, Germany) in order to keep constant the external power for each of the four cadences. During each test, subjects had not to balance due to the rolls that prevents from bicycles movements (Figure 11). Seat to pedal distance was adjusted to 100% of trochanteric leg length in both bicycles.
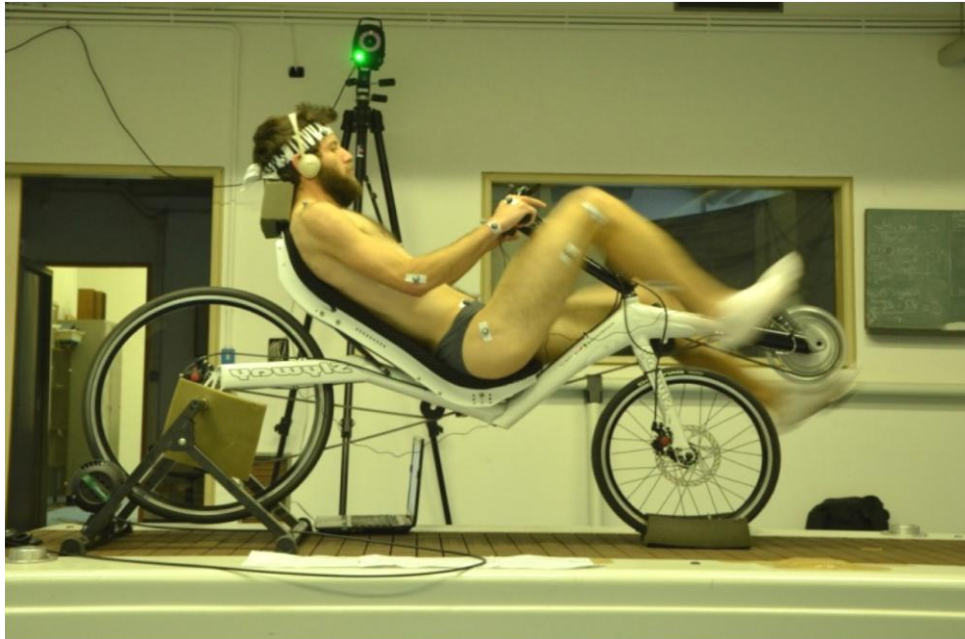
**Figure 11.** One typical subject during the experimental protocol.

3D kinematic data were obtained with a motion analysis system with 8 infrared cameras (Vicon MX, Oxford Metrics, UK) at a sampling rate of 100 Hz. 35 reflective markers (∅ = 14 mm) were positioned on subject's body landmarks according to Plug-In-Gate model like in figure 13 (Davis et al., 1991; Kadaba et al., 1990) in order to perform successively musculoskeletal modelling and two additional markers were placed in correspondence of the right and left greater trochanter for the computation of the BCoM. This protocol allowed us to analyze more than 2500 pedalling cycles.
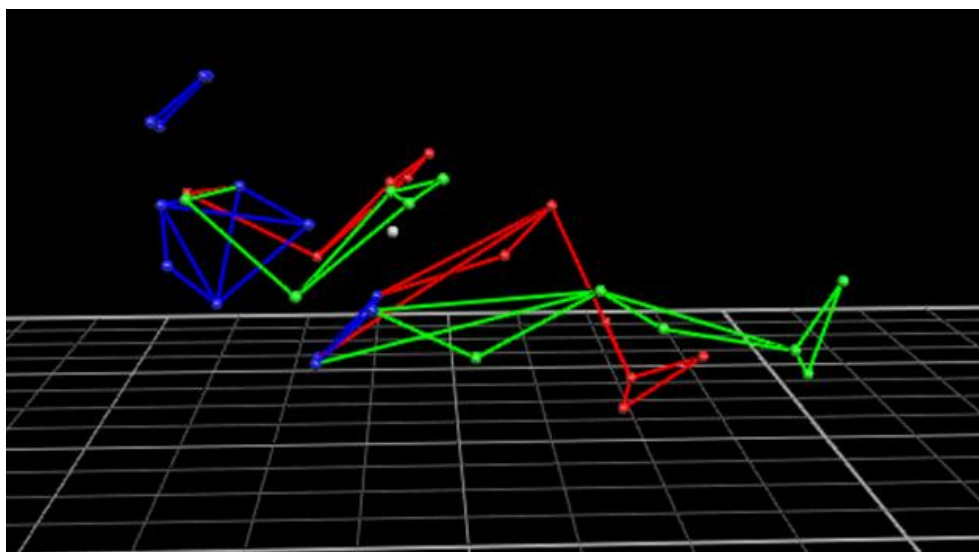


**Figure 12.** Sagittal view of a acquisition of VICON motion capture system with the plug in gate marker set. In This view the two marker in correspondence of the great trochanter, necessary for the BCoM analysis, are omitted.
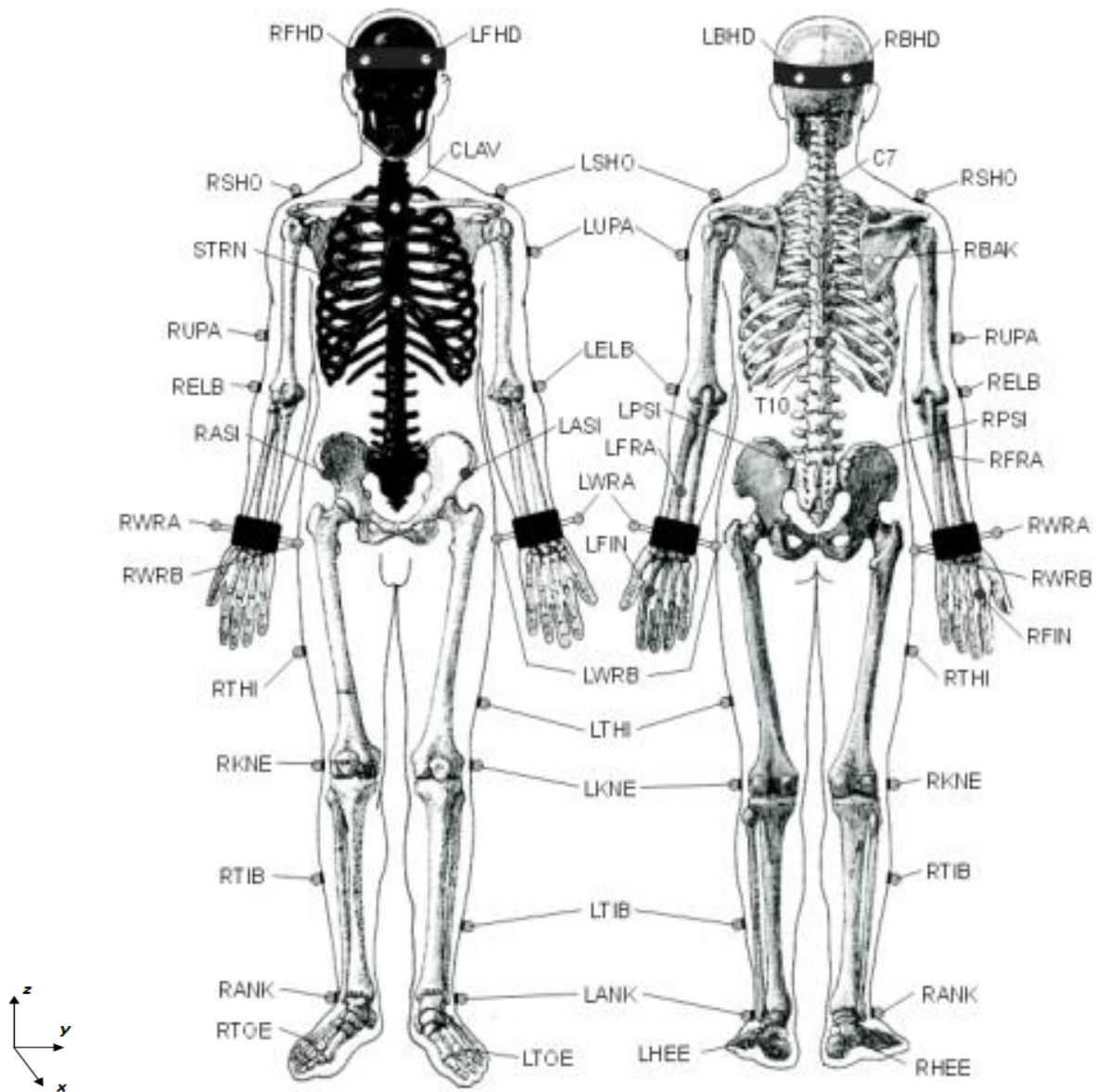
**Figure 13.** This image describes where the Plug-in-Gait markers should be placed on the subject. Here only the left side markers are listed, the positioning is similar for the right side. *LFHD* Left front head; *RFHD* Right front head; *LBHD* Left back head; *RBHD* Right back head; *LSHO* Left shoulder; LELB Left elbow; *LWRA* Left wrist; *LWRB* Left wrist; *LFIN* Left fingers; *LASI* Left ASIS; *LPSI* Left PSIS;  *KNE* Left knee; *LTHI* Left thigh; *LANK* Left ankle; *LTIB* Left tibia; *LTOE* Left toe; *LHEE* Left heel; *C7* 7th Cervical Vertebrae; *T10* 10th Thoracic Vertebrae; *CLAV* Clavicle; *STRN* Sternum; *RBAK* Right Back. LUPA Left upper arm and and LFRA Left forearm were not used.

Two other markers are not reported here but were attached in correspondence of the great trochanter for further analysis. The reference system we used is also reported: *x* for forward, *y* for lateral and *z* for vertical direction.

## 2.3 Bicycles technical data

The experiments were performed with a slyway hyper recumbent bicycle (SlyWay®; Slyway Project, Cremona, Italy) whose geometry is reported in Figure 14. Whereas on traditional recumbents the seat and back support are close to road level, on this chassis the rider sits higher (saddle height is 0.37 m from the ground).
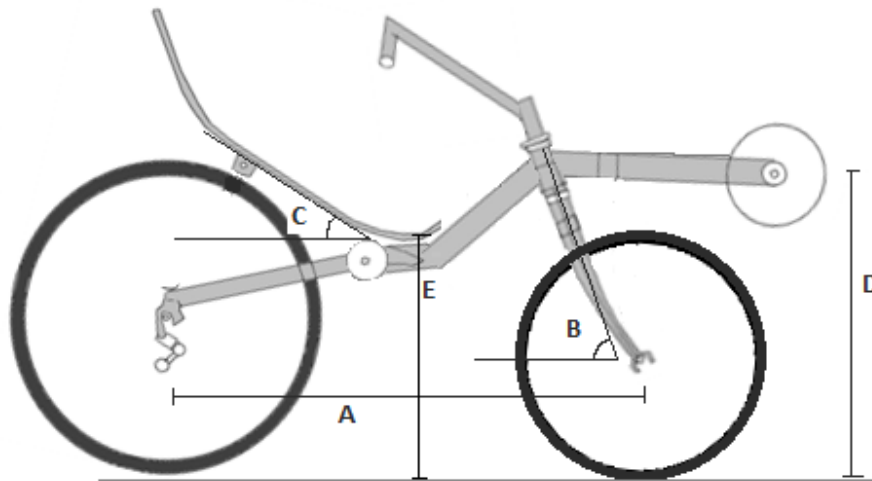


**Figure 14.** Main dimensions of the recumbent bicycle used during the experiments. Front wheel size 0.508 m; rear wheel size 0.660 m; wheel base (A): 1.23 m; head tube angle (B): 72°; seat angle (C): 30°; medium bottom bracket (D): 0.585 m; seat height (E): 0.370 m.

The experiments while riding a NB were performed with a velo route tribian 300 (B'Twin®; Dechatlon) whose geometry is reported in Figure 15.
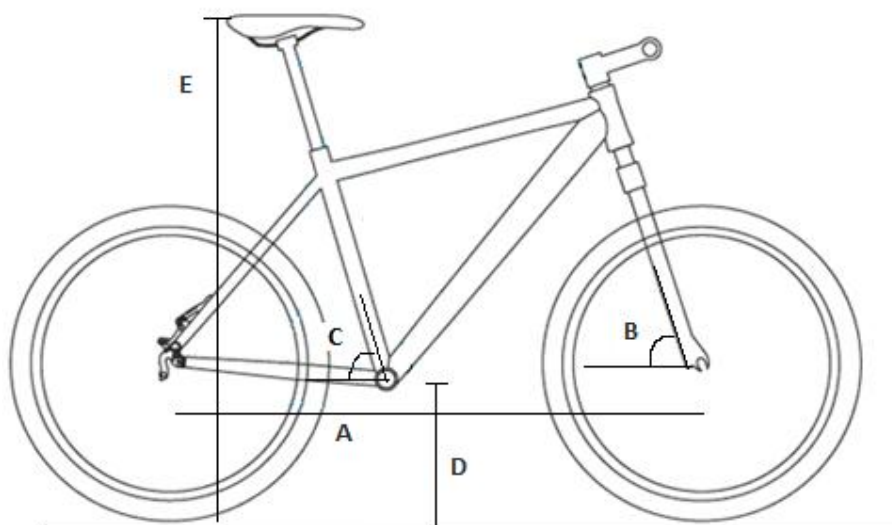


**Figure 15.** Main dimensions of the recumbent bicycle used during the experiments. wheel size 0.620 m. Wheel base (A): 1.42 m; head tube angle (B): 68°; seat tube angle (C): 75°; medium bottom bracket (D): 0.30 m; seat height (E): depending on the trochanteric le length of the subjects.

## 2.4 Position of the subjects

According to the nomenclature proposed in literature (Reiser, Peterson, & Broker, 2002) we evaluated the posture of the riders on the bicycles (figure 16). The angle with origin at the hip joint, formed by the trunk and the segment connecting the hip joint and the crank, called *Body Configuration* Angle (BC), was, on average, 123° ± 4° in NB and 143° ± 1°in RB. The *Hip Orientation* (HO), the angle of hip joint centre to bottom bracket relative to horizontal, was 75° ± 0° in NB and 0° ± 1° in RB while the *Torso Angle* (TA), referred to the angle between hip-shoulder segment and the horizontal line passing through the hip joint, was 133° ± 4 in NB and 36° ± 2° in RB. Thus, the change in posture in RB is not a homogeneous backward rotation of the whole body, resulting (for our bicycle model) a -75º rotation of the lower limbs with a further -20º backward rotation of the trunk, with a total range approximately of 100°. Seat to pedal distance (SPD) was adjusted to 100% of trochanteric le length as previously said. In this new bicycle configuration we could expect some changes of operative length of muscles crossing the hip joint.
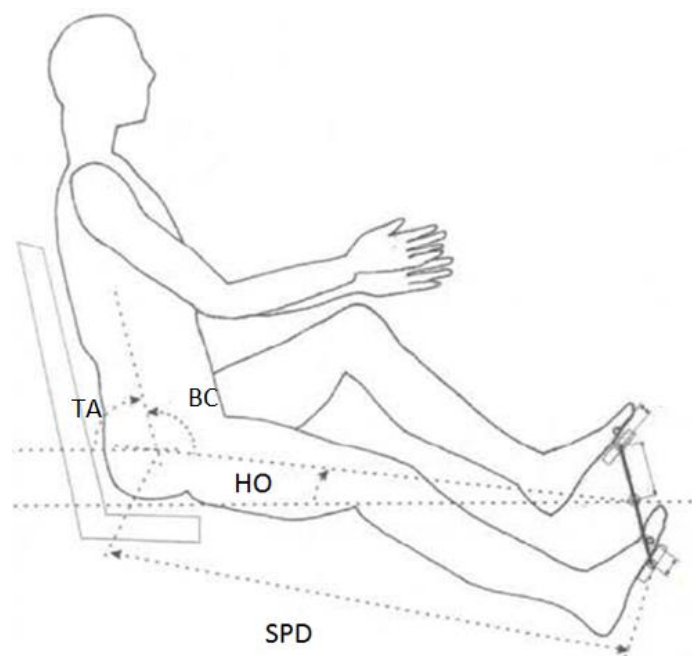


**Figure 16.** Geometrical variables describing the position of the riders on a bicycle are reported. HO: Hip Orientation; BC: Body Configuration Angle; SPD: seat to pedal distance; TA: Torso Angle. adapted from Reiser & Peterson, 1998.

# 2.5 Muscolo-Scheletal Modelling with OpenSim®

Movement is natural for most of us, it is necessary to meet people, go to work, play sport. Opensim® (Simbios, Stanford University) can help scientist allowing them to create very accurate human or animal models useful to understand the way they move. It is know that each muscle in the body generate a force pooling the bones connected to close together. Moreover, when activated, other muscles generate other forces and, consequently, may provide movement.

Using the knowledge of anatomy, physics and physiology it is possible to estimate all the forces generated by muscles and their activation and deactivation. In this way it is possible to reproduce and study kinetic and kinematics of movement. Opensim is wild used in different fields: clinicians may be interested in the diseases that affects muscles, bones and nerves making normal activity such running, walking or cycling not so simple. For example, some researchers are studying cerebral palsy patients (Steele et al., 2010, 2013) where the common movement pattern is called crouch gait, defined as excess flexion or bending of the knee joint during walking. The results of this works may help doctors that can analyze this gait and evaluate how to intervene. Planning treatment is just one of the application of Opensim, indeed it is used in biomechanics research, ergonomic analysis and design, sports science, robotics research, biology, and education.

In locomotion field it allowed to analyze muscles coordination, forces and function during walking (Xiao & Higginson, 2007, 2010; Liu et al., 2008) and running (Hamner et al., 2010). Simulating motions may have different objectives, in this study our interest is to analyze the cyclist course of motions to evaluate differences between two cycling condition and to lead him to better results in competitions.

Summarizing, OpenSim is an open-source software that enables users to build and analyze computer models of the musculoskeletal system and dynamic simulations of movement. In this thesis Opensim will be used to create subject-specific models of motion, analyze the experimental data captured from the VICON motion capture system and estimate the muscle tendon length with a purely kinematic analysis, whose validity is a function of the model biofidelity.

## 2.6 Model Scaling

The first step to do when using Opensim is to alter the anthropometry of the generic model so that it matches a particular subject characteristics as closely as possible by using the Scale Tool. Scaling can be performed using a combination of two methods:

- *Measurement-based Scaling*: the "scale factor" is determined by the relative distance between two specified *experimental marker* (blue marker on figure 17) and the corresponding *virtual markers* (pink marker of figure 17) position. For each body segment, a single scale factor is computed using one or more marker pairs. The pairs of markers selected for this purpose are presented in figure 18.

- *Manual Scaling*: the scale factor of this kind of scaling is predetermined by the user. This methods can be necessary when marker data are not available.

In addition, the masses of the segments are adjusted so that the total mass of the body equals the specified subject mass.
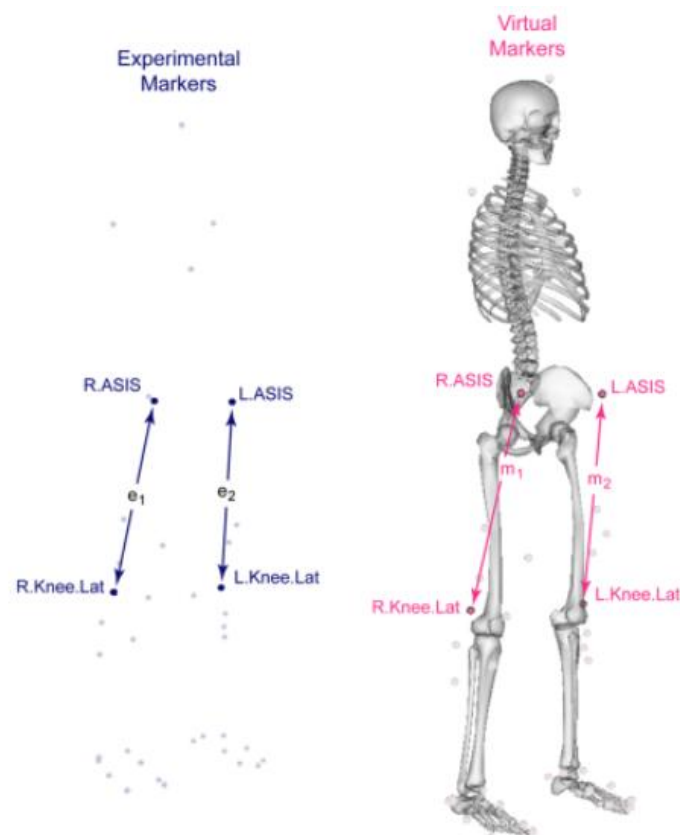


**Figure 17.** The experimental (blue) and virtual (pink) markers are used to scale the generic model.

**Figure 18.** Pairs of markers used to scale the different body segment of the general model. The nomenclature of the different markers is in line with the Plug-In-Gate markerset.

The Scale Tool needs mainly three file to finish the process and generate the scaled model (figure 19), and  is essential for getting good results from Inverse Kinematics:

Subject01_static.trc: "*experimental marker*" trajectories for a static trial containing several seconds of data with the subject posed in a known static position.

Subject_model.osim: OpenSim musculoskeletal model selected for the experiments. This generic model will be scaled to match the subjects anthropometry.

Subject_markerSet.xml: contain the markerset used in the experimental protocol and correspond to the "*virtual markers*".
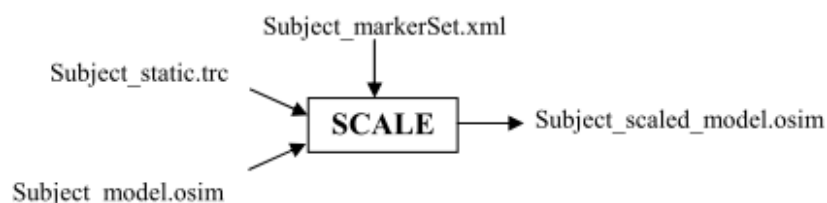


**Figure 19.** Required inputs and output for the Scale Tool.

# 2.7 Inverse Kinematic

With the Inverse Kinematics Tools the experimental markers are matched by model markers throughout the motion by varying the joint angles (generalized coordinates) through time (figure20). This allow to find the coordinate for the model  that  "best  matches" experimental marker position and coordinate data recorded during each experimental trial. This "best match" is the pose  that minimizes a sum of weighted squared errors of markers and/or coordinates. In other words it minimizes the difference between the experimental

33

marker location and the model's virtual marker locations. Therefore, in each frame of the experimental data, the weighted squared error is minimized.

The operator can differently weight the markers during the weighted least squares minimization operation: larger weightings penalize errors for that marker or coordinate more heavily and thus should match the experimental value more closely. For example, bony landmarks (i.e. knees, ankles, anterior superior iliac spine) had greater weightings than fleshy landmarks (i.e. thighs or calves) because the degree of certainty for correct marker placement is higher. When the weighted squared error is minimized, the coordinate values which produced this error are reported for the frame. The required inputs and outputs for the Inverse Kinematic Tool is reported in figure 21.
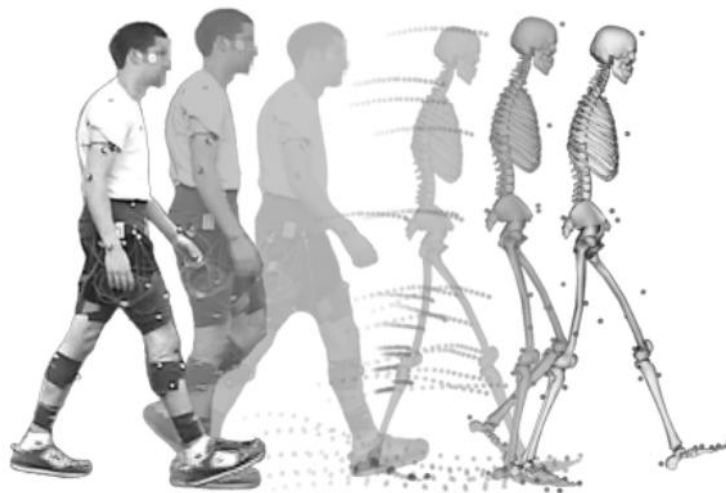


**Figure 20.** The Inverse Kinematic Tool is necessary to build and analyze computer models of the musculoskeletal system starting from the experimental markers applied on the subject.
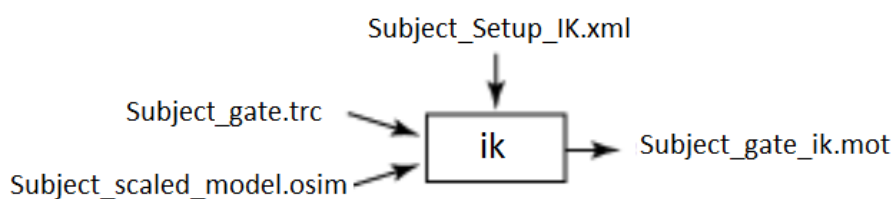


**Figure 21.** Inverse Kinematic Tool (ik) needs 3 input to be completed: "Subject_scaled_model.osim": a subject-specific OpenSim model generated by scaling a generic model with the Scale Tool; "Subject_gate.trc": experimental marker trajectories for a trial obtained from our VICON motion capture system; "Subject_Setup": a file containing all the settings information for the IK tool, including marker weightings (IK tasks). When inverse kinematic tool is completed a motion file containing the generalized coordinate trajectories (joint angles and/or translations) will be computed " Subject_gate.mot:".

The results of Scaling and Inverse Kinematic Tools were evaluated following the guideline of OpenSim: maximum marker error and RMS error were always less than 2 and 1 cm respectively during the Scaling and less than 4 and 2 cm during the Inverse Kinematic Tools.

## 2.8 Estimation of Muscle-Tendon Length and Joint Angle

Muscle–tendon lengths are determined solely by the positions of muscle origins, insertions, and any path defining waypoint or wrapping surfaces. That is, it is a purely kinematic analysis, whose validity is a function of the model biofidelity. For this reason lower limbs muscle-tendon length (MTL) were estimated with the musculoskeletal modelling software OpenSim 2.4. (Delp et al., 2007) because this software include a algorithm well-accepted in the biomechanics community for computing muscle-tendon length.

Subject's body mass together with the 3D markers coordinates of the static trial obtained from kinematical recordings were used to match the specific subject's anthropometry and scale the Gait2392_Simbody model which includes 23 degrees of freedom and 92 muscle–tendon units. Successively, the inverse kinematics tool of OpenSim was used to compute joint angles of the scaled model that best reproduced subject's motion. For one trial each of cycling in NB and RB, approximately 60 s of marker position data were used to drive the inverse kinematic analysis. We analyzed the most involved muscle-tendon units (MTU) in pedalling cycles: gluteus maximus, vastus lateralis, medialis and intermedius, rectus femoris, soleus, medial and lateral gastrocnemius, tibialis anterior, biceps femoris longus and brevis, iliacus, psoas. Data where exported in .txt file from the OpenSim plot tool. All MTL were computed but, similarly to other studies (Sanderson et al., 2006; Austin et al., 2010) we have analyzed only one side. The MTL data presented in this thesis are normalized to the standing length (MTL of the same muscle during the static trial, when the subject was in a standing position).

We analyzed different joint angles computed with OpensSim including: lumbar extension, lumbar bending, lumbar rotation, hip flexion, hip adduction, knee angle and ankle angle. Lumbar extension, bending and rotation are the angle between the pelvis and the trunk.

The transformation between the pelvic and femoral reference frame is determined by successive rotations of the femoral frame about three orthogonal axes fixed in the femoral

head. The angle between pelvis and femur frame gives origin to Opensim hip_flexion that have a value of zero when the subject is in the anatomical position and ranges from -120 to +120 when the leg is extended or flexed respectively. Opensim knee_angle is the angle between shank and thigh and ranges from -120 (knee flexed) to +10 (knee extended), while Opensim ankle_angle have a value of 0 in neutral position and ranges from -90 (full plantar-flexion) to +90 (full dorsi-flexion).

In this work these angles have been changed as proposed in figure 22: Hip Angle was set with a value of 180° in standing position and varies from 60° when flexed (60° between pelvis and femour and corresponding to a value of -120° when using Opensim hip_flexion) to 300° (corresponding to a value of +120° when using Opensim hip_flexion) when extended.

Knee Angle have a value of 180° when extended, 190° in the in model maximal extension (hyperextension), and 60° at the model maximal flexion (corresponding respectively to +10° and -120° when using Opensim reference values).

Ankle Angle ranges from 0° (full dorsi flexion) to 180° (full plantar flexion) and is 90° in standing position.

Starting from the data exported from the plot tool, we elaborated a custom program written in Labview in order to calculate the maximum, minimum and the range of movement of the computed muscles and joint angles.
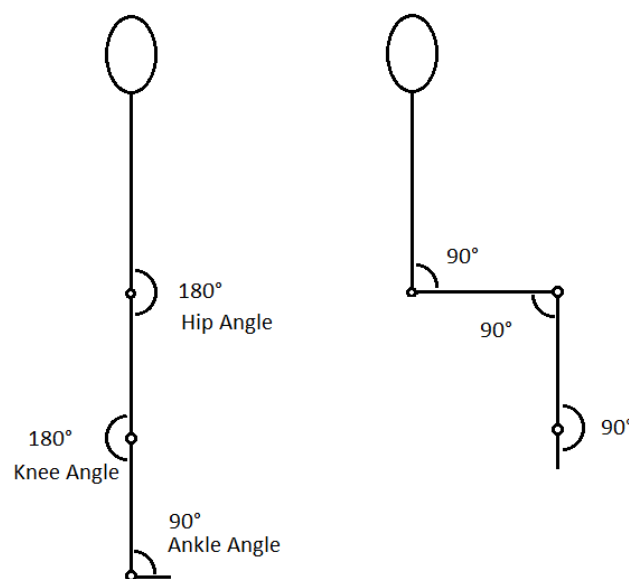


**Figure 22.** Joint angle definition proposed in this thesis. In the left side was reported the standing position where Hip, Knee and Ankle angle had a value od 180°, 180° and 90° respectively. In the right side we reported a different position to show how varying the joint angles.

## 2.9 Body Centre of Mass analysis

According to previous studies on different locomotion types (Minetti et al.,1993; Minetti et al., 2012; Seminati et al., 2013) we selected 18 of the 37 markers in order to detect 12 body segments. Their fractional mass, Centre of Mass and the moment of inertia (Winter, 1979) were used to determine the 3D position of the BCoM and the linear and angular speed of segments at each frame. The trajectory of the BCoM has been described with a Lissajous contour, a convoluted loop showing its 3D displacement with respect to the average position. This parametric representation of BCoM trajectory allows to obtain closed loops for the body centre of mass showing some characteristics typical of the locomotion. Indeed, this path describes both its kinematical and dynamical features and was obtained by applying the mathematical framework proposed by Minetti et al. (2011) based on Fourier analysis. This procedure allows computing also the Symmetry Indices (SI) of the BCoM along the 3 spatial axes and they are expected to be equal to 1 in case of perfect symmetry between right and left pedalling.

Starting from the body segments and the 3D position of the BCoM we could evaluate the mechanical work done associated to their movement (Wext* and $\dot{W}_{INT}$). To do that, it is necessary to calculate the total mechanical energy of the BCoM (TE), which is the sum of the potential energy (PE), directly proportional to vertical position of BCoM, and kinetic energy (KE), directly proportional to the square of speed. In this work, PE and Kinetic Energy on antero-posterior (KEx), vertical (KEz) and medio-lateral (KEy) axes were measured with a custom program written in LabView (ver. 8.6 National Instruments) (Minetti, 1998).

$\dot{W}_{EXT*}$ was computed as the ratio between the sum of positive changes of the total mechanical energy (TE=PE+KEx+KEz+KEy) of BCoM (when the speed of progression is considered 0) during the pedalling cycle and the time of pedal revolution. Since our subjects cycled on rollers their speed of progression was 0, this allowed us study the Wext* of BCoM by excluding the velocity.

$\dot{W}_{INT}$ was calculated as the sum of kinetic linear and angular energies of the segments relative to the BCoM (Cavagna & Kaneko 1977; Minetti, 1998) and $\dot{W}_{EXT}$ was directly measured from the SRM.

## 2.10 Physical simulation of pedalling cyclist

As previously mentioned, this study is conducted by means of double approach: experimental and theoretical. In this paragraph will be presented a dynamical simulation of a pedalling cyclist (Working Model 2D, Design Simulation, US). The subject (75 kg body mass) was modelled with rectangular segments, with a mass of 51, 7.5 and 4.5 kg respectively for trunk, thigh and shank. The first segment represent the Trunk-Head-Arm segment and is about the 68% of the total mass (the sum of Total Arm, Head and Neck and Trunk segment as reported in table 2). The Thigh and Shank segments are respectively 10 and 6 % of the total mass in accordance to the anthropometric data present in literature (DA Winter, Biomechanics and Motor Control of Human Movement, 3rd edition) and are connected together by frictionless pin joints. The distal portion of the tibias was attached to a chain ring where a motor allowed the movement with imposed angular speed corresponding to 50, 70, 90 and 110 rpm. This simulation allowed us to calculate the velocity and trajectory of BCoM in sagittal plane, $\dot{W}_{EXT^*}$, $\dot{W}_{INT}$ and the angular speed of pedal. The gait cycle started when the pedals were perpendicular (in NB) or parallel (in RB) to the ground.

Normalized Mass and Length of Body Segments (Standard Human)

| Segment | Segment Mass / Total Body Mass | Center of Mass / Segment Length Proximal | Distal | Density (kg/l) |
|---|---|---|---|---|
| Hand | 0.006 | 0.506 | 0.494 | 1.16 |
| Forearm | 0.016 | 0.430 | 0.570 | 1.13 |
| Upper Arm | 0.028 | 0.436 | 0.564 | 1.07 |
| Forearm and Hand | 0.022 | 0.682 | 0.318 | 1.14 |
| Total Arm | 0.050 | 0.530 | 0.470 | 1.11 |
| Foot | 0.0145 | 0.500 | 0.500 | 1.10 |
| Lower Leg (calf) | 0.0465 | 0.433 | 0.567 | 1.09 |
| Foot and Lower Leg | 0.061 | 0.606 | 0.394 | 1.09 |
| Upper Leg (thigh) | 0.100 | 0.433 | 0.567 | 1.05 |
| Total Leg | 0.161 | 0.447 | 0.553 | 1.06 |
| Head and Neck | 0.081 | 1.000 | — | 1.11 |
| Trunk | 0.497 | 0.500 | 0.500 | 1.03 |

Adapted from DA Winter, *Biomechanics and Motor Control of Human Movement*, 3rd edition (John Wiley & Sons 2005)

**Table 2**. In the table are reported different anthropometric characteristics used to model our subjects. We relied on data in the second column (Segment Mass / Total Body Mass) to calculate the specific mass for each single segment of the pedalling cyclist model.

Figure 23 shows all the output of the model that we have analyzed. Clockwise from upper left, the output windows show instant values of variables related to:

- the position of the BCoM

- the energies associated to the BCoM and the crank

- the velocity of BCoM

- the velocity of each segment respect to the velocity of BCoM

- the power needed to the motor to rotate the system

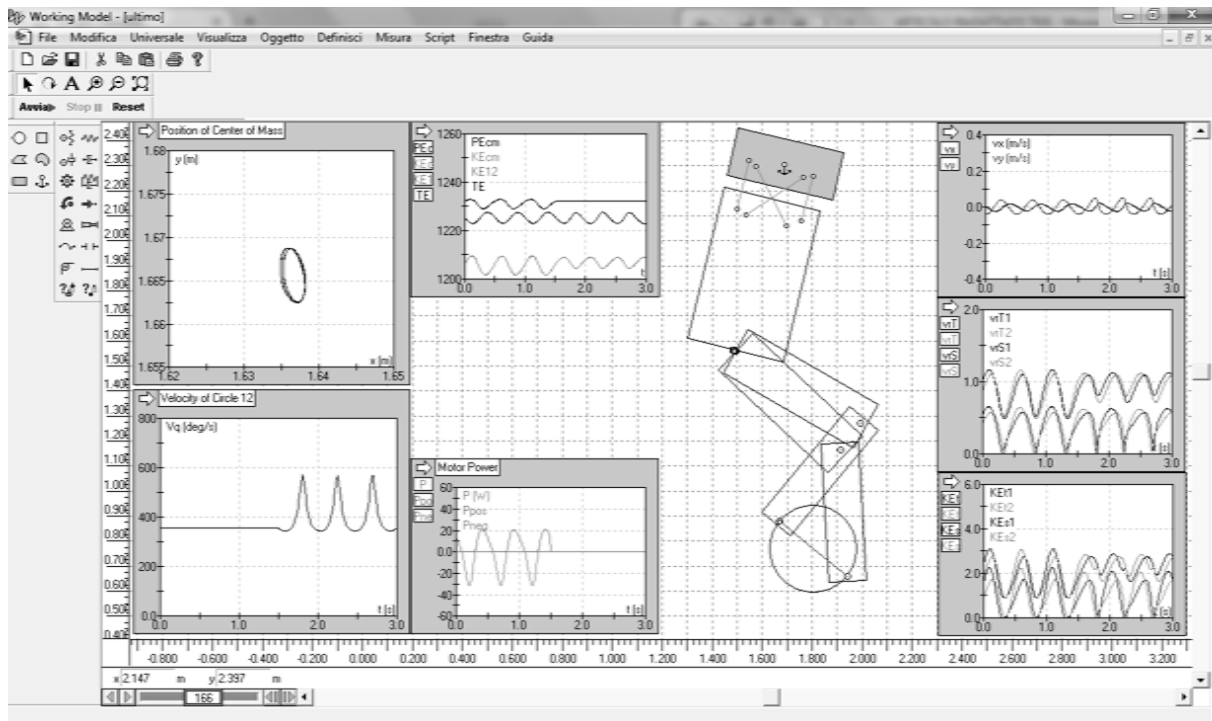- the angular velocity of the crank



**Figure 23.** Working Model Simulation of pedalling cyclist.

## 2.11 Statistical analysis

To evaluate the effect of different pedalling cadence (independent variable) a one-way ANOVA for repeated measures with a post-hoc Bonferroni test was performed on the following parameters: BCoM excursion, symmetry indices on tree different spatial axes (SIx, SIy, SIz respectively for antero-posterior, medio-lateral and vertical direction), $\dot{W}_{INT}$ and $\dot{W}_{EXT^*}$. The test has been performed both for NB and RB separately. In addition, differences between the two bicycles were analyzed using a paired t-test at each of the selected cadences for each of the previously listed parameter. With the hypothesis that cadence has no effects on MTL, we compared the behaviour of each analysed muscles in the different bicycles with a paired t-test without taking into account the different rpm. Statistical significance was accepted when $p < 0.05$.

# CHAPTER THREE

# Results

## 3.1 Joint Angle and Muscle-Tendon Length

The comparison of hip, knee and ankle angles, averaged for all the pedalling frequencies highlights the differences in movement of these joints. hip, knee and ankle joints motion during the pedal cycle (from 0° to 360°), together with lumbar bending, are reported in figure 24. Full joint extension correspond to an angle of 180° for the first three angles but not for lumbar bending.
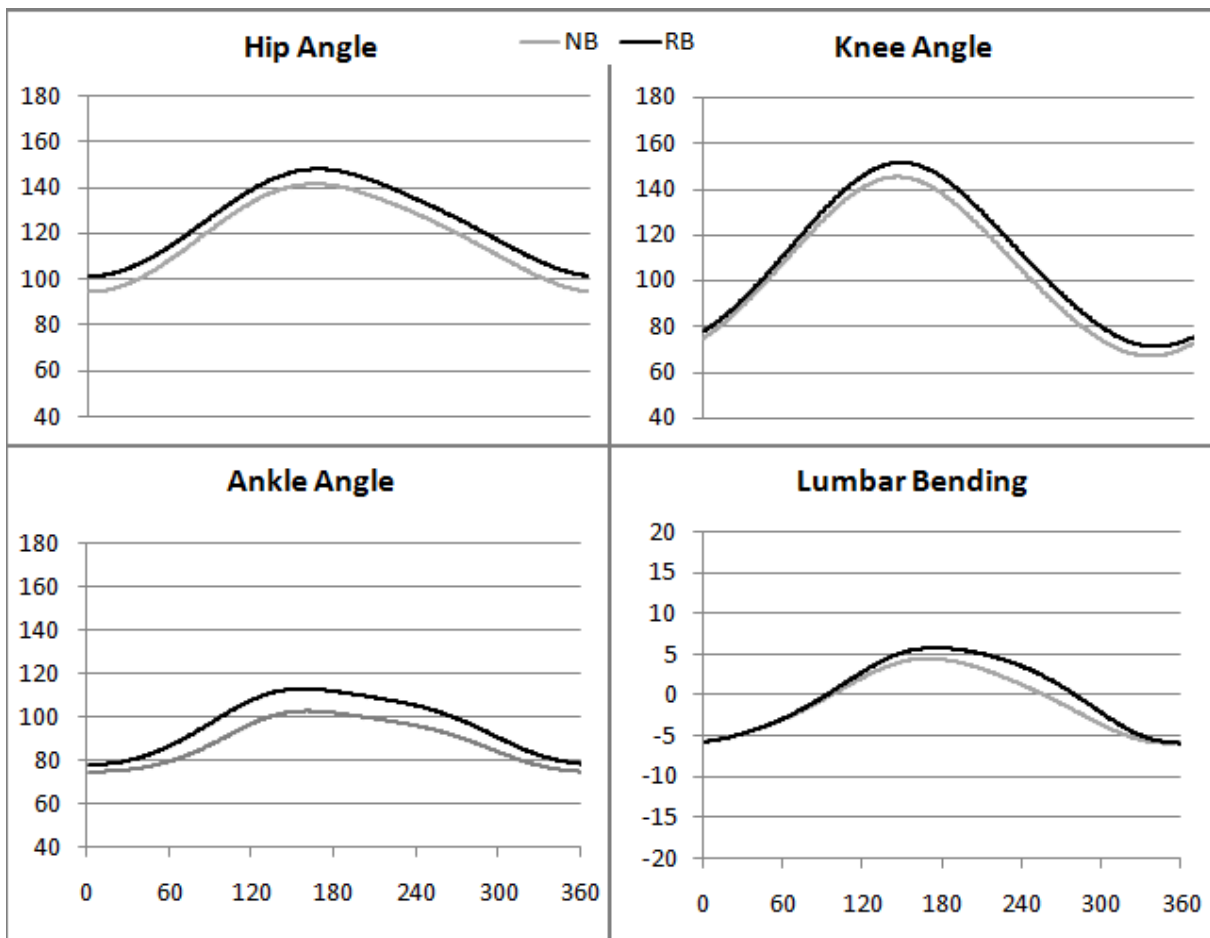


**Figure 24.** Comparison between Joint angles (°) of the left lower leg and of the trunk over a complete crank cycle in NB and RB. In this graphs the black and grey lines represent the average value for all the pedalling frequencies.

Table 3 indicate maximum (Max), minimum (Min) and range of motion (Exc) of different joint for all pedalling cadences and bicycle position. The range of motion of the left ankle (23.1 in NB and 36.2 in RB) is lower than heather the left hip (48.2 in NB and 46.9 in RB) and knee (78.2 in NB and 81.7 in RB). Similar values are reported also in the right joints.

| | | 50 RPM | | 70 RPM | | 90 RPM | | 110 RPM | |
|---|---|---|---|---|---|---|---|---|---|
| | | NB | RB | NB | RB | NB | RB | NB | RB |
| L_ext | Max | -45.7±8.9 | -26.7±3.0 | -45.7±9.0 | -26.7±4.2 | -45.7±8.4 | -27.4±4.1 | -45.7±11. | -27.4±4.4 |
| | Min | -46.7±9.1 | -27.8±2.0 | -46.8±8.9 | -27.5±4.3 | -46.7±8.1 | -28.3±4.5 | -46.7±11. | -28.3±3.7 |
| | Exc | 1.1±0.4 | 1.1±0.2 | 1.1±0.5 | 0.8±0.3 | 1.0±0.3 | 0.9±0.2 | 1.0±0.4 | 0.8±0.2 |
| L_bend | Max | 4.2±1.6 | 6.7±3.5 | 3.7±1.2 | 4.0±1.7 | 4.8±1.3 | 5.4±1.6 | 4.8±2.1 | 5.4±3.4 |
| | Min | -5.2±0.6 | -5.0±1.8 | -6.0±1.2 | -5.7±1.9 | -6.0±0.9 | -6.4±1.7 | -6.0±1.1 | -6.4±1.4 |
| | Exc | 9.5±0.8 | 11.9±1.1 | 9.8±0.7 | 9.8±0.9 | 10.9±0.5 | 11.9±0.8 | 11.4±0.6 | 13.3±0.9 |
| L_rot | Max | 1.4±0.6 | 5.8±3.5 | 1.5±1.9 | 2.5±1.9 | 0.7±0.7 | 1.7±3.2 | 0.7±1.5 | 1.7±2.5 |
| | Min | -2.5±2.0 | 2.9±3.1 | -1.9±2.7 | 0.95±1.9 | -2.9±3.3 | -0.0±4.6 | -2.9±2.5 | -0.0±2.2 |
| | Exc | 3.9±0.6 | 2.9±0.5 | 3.5±0.9 | 1.6±0.7 | 3.7±0.4 | 1.8±0.5 | 6.7±0.6 | 2.5±0.5 |
| Hip L | Max | 142.7±5.8 | 148.4±3.0 | 142.1±7.0 | 148.4±4.9 | 141.5±6.4 | 146.6±4.4 | 141.5±9.1 | 146.6±3.3 |
| | Min | 94.5±6.7 | 101.5±3.3 | 94.5±6.3 | 100.9±4.0 | 94.5±6.1 | 100.5±4.6 | 94.5±7.4 | 100.2±3.4 |
| | Exc | 48.2±4.1 | 46.9±4.2 | 47.6±4.1 | 47.6±3.9 | 46.9±4.3 | 46.1±4.0 | 45.6±4.5 | 46.3±3.6 |
| Knee L | Max | 145.8±6.7 | 151.8±3.3 | 144.7±8.8 | 153.4±3.1 | 143.8±6.3 | 150.3±3.9 | 143.8±9.9 | 150.3±1.5 |
| | Min | 66.7±5.1 | 71.4±2.3 | 66.5±5.9 | 71.6±2.5 | 66.4±5.3 | 70.6±1.4 | 66.4±8.9 | 70.6±1.2 |
| | Exc | 79.1±5.6 | 80.3±5.1 | 78.2±5.7 | 81.7±4.7 | 77.5±5.2 | 79.7±4.6 | 77.8±5.6 | 79.3±5.6 |
| Ank L | Max | 98.8±2.6 | 114.1±4.1 | 102.5±2.8 | 112.7±3.2 | 102.9±2.3 | 112.1±4.1 | 102.9±2.3 | 112.1±4.1 |
| | Min | 75.7±4.7 | 77.9±3.5 | 75.8±3.7 | 78.6±4.1 | 74.3±3.5 | 77.8±4.8 | 74.3±6.0 | 77.8±5.0 |
| | Exc | 23.1±2.2 | 36.2±3.5 | 26.7±2.5 | 34.1±3.2 | 28.7±2.8 | 34.3±3.7 | 33.9±2.7 | 34.9±3.2 |
| Hip R | Max | 144.2±5.9 | 149.2±2.1 | 142.9±6.7 | 148.6±5.2 | 141.8±5.1 | 148.2±4.6 | 141.8±8.6 | 148.2±3.5 |
| | Min | 94.6±7.9 | 101.6±2.4 | 94.2±8.4 | 99.8±5.6 | 94.1±7.4 | 100.±3.4 | 94.1±8.8 | 100.±2.7 |
| | Exc | 49.6±3.4 | 47.6±3.3 | 48.7±3.2 | 48.8±3.6 | 47.7±3.2 | 48.2±3.4 | 48.0±3.3 | 47.8±3.4 |
| Knee R | Max | 148.4±5.7 | 154.3±3.3 | 146.0±6.8 | 154.2±3.2 | 145.0±4.5 | 153.2±2.9 | 145.0±9.7 | 153.2±2.0 |
| | Min | 65.9±4.7 | 70.5±1.7 | 65.2±5.3 | 70.5±2.1 | 65.3±4.1 | 69.6±2.0 | 65.3±8.9 | 69.6±0.9 |
| | Exc | 82.6±5.4 | 83.8±4.8 | 80.7±5.3 | 83.8±4.9 | 79.6±5.6 | 83.6±4.8 | 79.7±5.6 | 82.7±5.8 |
| Ankle R | Max | 99.1±3.5 | 115.4±4.0 | 102.±3.0 | 114.3±3.3 | 104.±3.1 | 114.3±4.9 | 104.±3.2 | 114.3±5.1 |
| | Min | 75.6±7.0 | 78.5±4.8 | 77.0±6.1 | 80.2±3.3 | 76.6±3.4 | 79.2±3.3 | 76.6±7.0 | 79.2±3.8 |
| | Exc | 23.5±2.3 | 36.9±3.6 | 25.2±2.3 | 34.0±3.2 | 27.4±2.6 | 35.1±3.4 | 32.8±2.5 | 36.1±3.3 |

**Table 3.** Maximum, minimum and range of motion (°) of different joint angle L_ext, lumbar extension; L_bend, lumbar bending; L_rot, lumbar rotation; Hip L, left hip angle; Knee L, left knee angle; Ankle L, left ankle angle; Hip R, right hip angle; Knee R, right knee angle; Ankle R, right ankle angle for both bicycle and all pedalling cadences analyzed.

Results regarding MTU estimated with Opensim simulations are reported in term of percentage of the standing length (Table 4).

| Normal Bicycle | | | | | | |
|---|---|---|---|---|---|---|
| MTU | Max | DS | Min | DS | Excursion | DS |
| **Biceps Femoris Longus** | 107.0 | 1.7 | 102.3 | 1.0 | 4.7 | 0.7 |
| **Biceps Femoris Brevis *** | 91.9 | 2.5 | 76.7 | 0.7 | 15.2 | 2.0 |
| **Gluteus Maximus *** | 129.2 | 1.2 | 116.9 | 2.3 | 12.4 | 1.7 |
| **Iliacus *** | 85.9 | 3.0 | 71.1 | 1.1 | 14.7 | 1.7 |
| **Lateral Gastrocnemius** | 96.3 | 1.0 | 93.4 | 0.9 | 2.9 | 1.2 |
| **Medial Gastrocnemius** | 96.3 | 1.1 | 93.3 | 1.0 | 3.0 | 1.3 |
| **Psoas *** | 88.9 | 2.2 | 77.9 | 0.9 | 11.0 | 1.3 |
| **Rectus Femoris** | 103.9 | 1.9 | 98.5 | 1.9 | 5.4 | 1.0 |
| **Sartorius *** | 91.7 | 1.9 | 77.3 | 0.7 | 14.4 | 1.8 |
| **Semimembranosus** | 103.9 | 2.2 | 97.8 | 1.0 | 6.1 | 0.8 |
| **Semitendinosus** | 104.5 | 2.3 | 98.3 | 1.0 | 6.2 | 0.8 |
| **Soleus *** | 102.2 | 1.0 | 95.8 | 1.6 | 6.4 | 1.5 |
| **Tibialis Antirior *** | 105.0 | 1.4 | 97.6 | 1.5 | 7.4 | 1.3 |
| **Vastus Intermedius *** | 137.2 | 2.0 | 114.6 | 3.4 | 22.7 | 3.7 |
| **Vastus Lateralis *** | 133.0 | 1.8 | 112.8 | 3.0 | 20.2 | 3.2 |
| **Vastus Medialis *** | 138.2 | 2.1 | 114.5 | 3.3 | 23.7 | 3.5 |
| Recumbent Bicycle | | | | | | |
| MTU | Max | DS | Min | DS | Excursion | DS |
| **Biceps Femoris Longus** | 106.3 | 1.2 | 101.6 | 1.3 | 4.7 | 0.4 |
| **Biceps Femoris Brevis** | 94.2 | 1.8 | 77.1 | 0.6 | 17.1 | 2.0 |
| **Gluteus Maximus** | 128.2 | 1.7 | 114.3 | 2.4 | 13.9 | 1.2 |
| **Iliacus** | 88.8 | 2.2 | 73.4 | 2.1 | 15.4 | 1.3 |
| **Lateral Gastrocnemius** | 95.6 | 1.4 | 92.4 | 1.7 | 3.2 | 1.4 |
| **Medial Gastrocnemius** | 95.6 | 1.4 | 92.3 | 1.7 | 3.2 | 1.4 |
| **Psoas** | 91.1 | 1.7 | 79.6 | 1.8 | 11.5 | 1.0 |
| **Rectus Femoris** | 104.5 | 1.5 | 98.5 | 1.3 | 6.0 | 0.7 |
| **Sartorius** | 93.7 | 1.4 | 79.0 | 1.3 | 14.7 | 1.3 |
| **Semimembranosus** | 103.9 | 1.3 | 97.5 | 0.9 | 6.4 | 0.8 |
| **Semitendinosus** | 104.4 | 1.5 | 97.9 | 1.1 | 6.5 | 0.7 |
| **Soleus** | 101.5 | 1.7 | 93.3 | 1.5 | 8.2 | 1.3 |
| **Tibialis Antirior** | 107.6 | 1.4 | 98.8 | 0.8 | 8.8 | 1.4 |
| **Vastus Intermedius** | 136.7 | 1.5 | 111.5 | 1.9 | 25.2 | 2.4 |
| **Vastus Lateralis** | 132.5 | 1.3 | 110.2 | 1.6 | 22.3 | 2.1 |
| **Vastus Medialis** | 137.6 | 1.6 | 111.5 | 1.9 | 26.0 | 2.4 |

**Table 4.** Maximal and Minimal MTL (% of resting length) reached by different Muscle Tendon Unit (MTU) in RB and NB; the difference between maximal and minimal MTL reached is the range of contraction of the MTU and is reported as 'excursion'. * indicate significant difference between bicycles ($p < 0.05$).

The middle point of contraction was also calculated (the average between maximal and minimal length reached during pedalling cycles) for each MTL, in order to understand whether that muscle was (on average) more elongated or shortened in one of the two positions. In RB, when compared to NB, Short Biceps Femoris (+1.3%), Iliacus (+2.6%), soleus (+1.6%) and Psoas (+1.9%) were more stretched; Gluteus Maximus (-1.8%), tibialis antirior(-1.9%) and the three Vasti (-1.8%) were shortened, while other muscles showed no differences (table 5).

| MTU | Mean NB | Mean RB | NB-RB |
|---|---|---|---|
| Biceps Femoris Longus | 104.6 | 104.0 | 0.7 |
| Biceps Femoris Brevis * | 84.3 | 85.7 | -1.3 |
| Gluteus Maximus * | 123.1 | 121.2 | 1.8 |
| Iliacus * | 78.5 | 81.1 | -2.6 |
| Lateral Gastrocnemius | 94.9 | 94.0 | 0.9 |
| Medial Gastrocnemius | 94.8 | 94.0 | 0.9 |
| Psoas * | 83.4 | 85.4 | -1.9 |
| Rectus Femoris | 101.2 | 101.5 | -0.3 |
| Sartorius | 84.5 | 86.4 | -1.9 |
| Semimembranosus | 100.8 | 100.7 | 0.2 |
| Semitendinosus | 101.4 | 101.1 | 0.2 |
| Soleus * | 99.0 | 97.4 | 1.6 |
| Tibialis Antirior * | 101.3 | 103.2 | -1.9 |
| Vastus Intermedius * | 125.9 | 124.1 | 1.8 |
| Vastus Lateralis * | 122.9 | 121.3 | 1.6 |
| Vastus Medialis * | 126.4 | 124.5 | 1.8 |

**Table 5.** Middle point of contraction reported as mean between Max and Min % of resting length reached by each MTU.

## 3.2 Dynamical Simulation of Pedalling Cyclist

As mentioned above, the pedalling task was due to the motor activity, but the chain ring continued to revolve even when the motor was switched off, showing a passive endless dynamics that occurred at fluctuating angular speed of the pedals (detail of Figure 25), in agreement with a previous work (Minetti, 2011). In this condition we identified two typical limbs configurations named P and λ, where the boundary of the major axis of the ellipse described by the BCoM are reached regardless the position of the subject. The analysis of freewheel cycling on NB at self selected pedalling cadence showed similarity with Working Model (WM) simulation: in the fluctuation of pedal crank angular velocity, higher speed values were recorded in P limbs configuration on both cases.
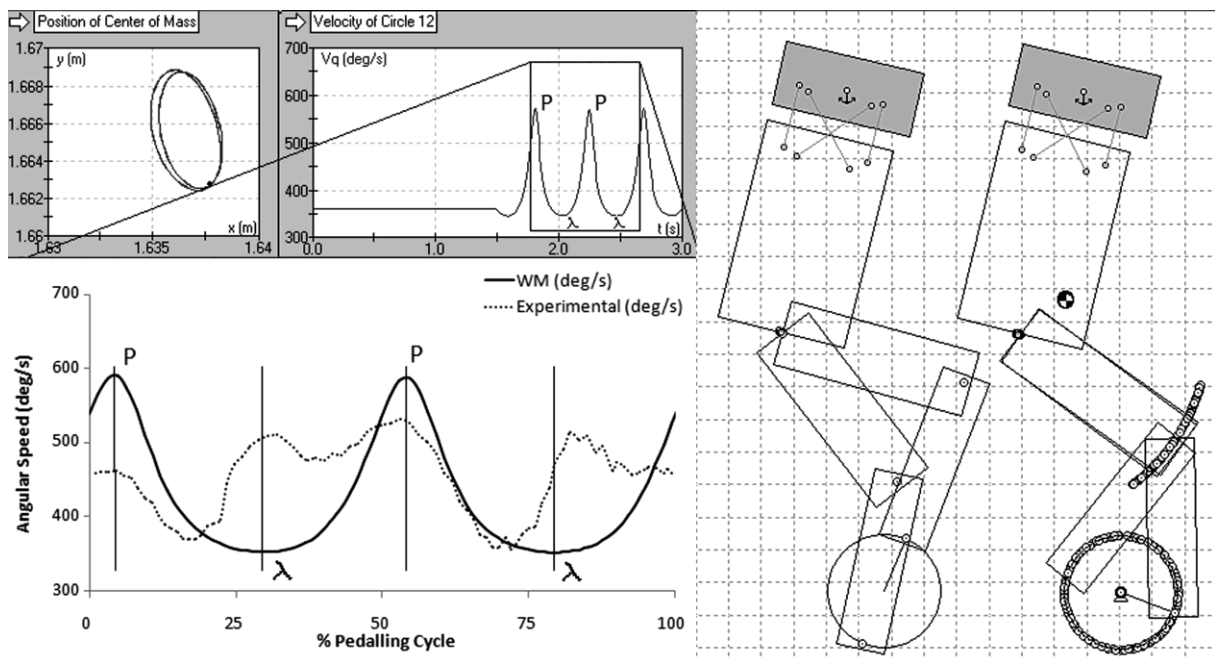


**Figure 25.** Working Model Simulation (WM) of pedalling cyclist on NB with limbs in P (on the left) and λ (on the right) configuration. Details regarding BCoM contour (sagittal plane) and velocity of the pedal are also appreciable in the left side of the figure.

## 3.3 Body Centre of Mass analysis

From 2D WM simulation we obtained also results regarding the 2D BCoM trajectory in sagittal plane, which described an elliptical profile with different major axis inclinations for the two bicycles. A similar behaviour was observed in the real path of the BCoM obtained from experimental sessions recordings (Figure 3). When one of the two lower limb segments in WorkingModel simulation (WM) is shortened replicating a common asymmetry in human body characteristics, the BCoM profile changes his shape (Figure 26A vs Figure 26B). We also reported examples of Lissajous contours of the BCoM of a typical subject while pedalling at 90 RPM on normal and recumbent bicycle (Figure 26D and 26E respectively).
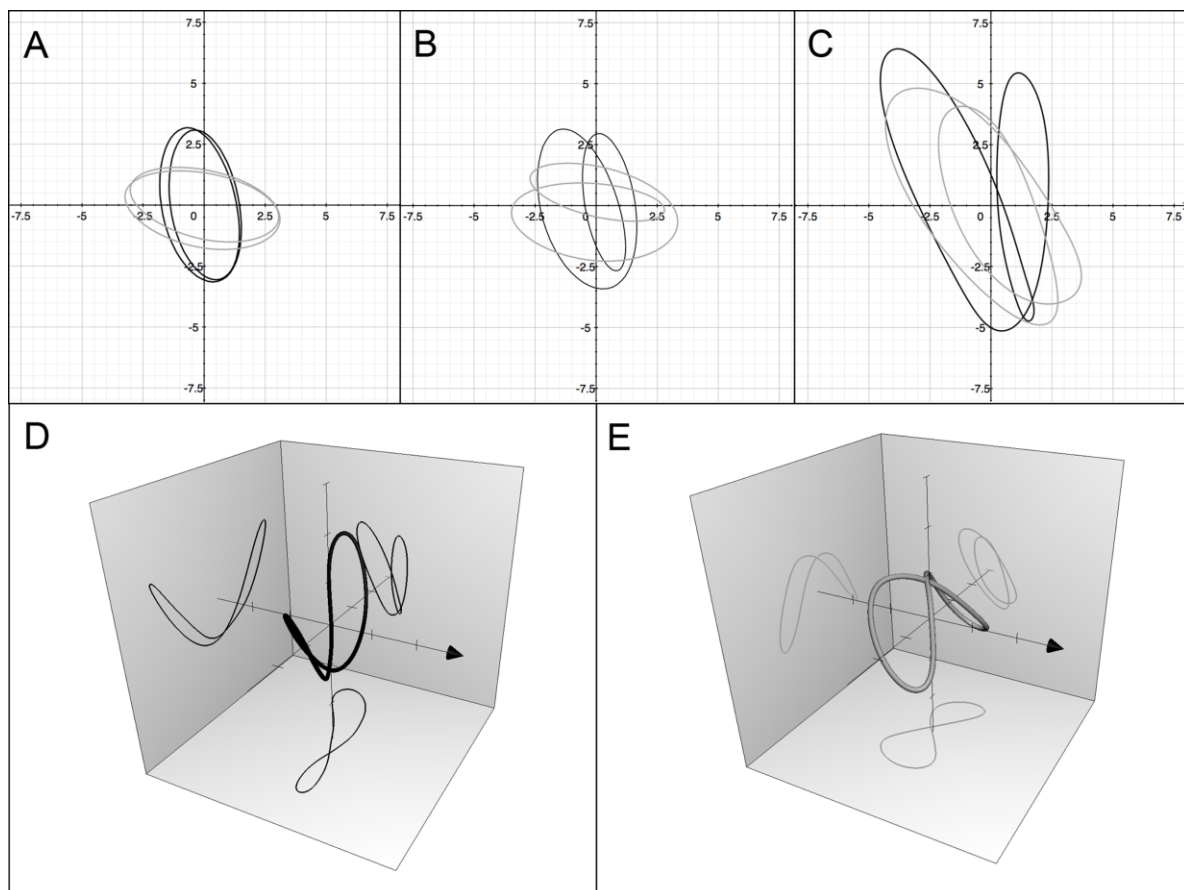


**Figure 26.** BCoM trajectories in the sagittal plane from Working Model symmetrical (A) and asymmetrical (B) simulation (one of the two tibia segments was shortened by 15 mm). The experimental contour in the same plane is also reported for a typical subject (C). Boxes D and E represent the 3D BCoM trajectories of the same subject respectively in NB (thick black line) and RB (thick grey line). Projections of the BCoM on the different planes (thin lines) are shown on the walls of the cube (side length 20 mm). The black arrow indicates the progression axis.

Even if the 3D BCoM trajectories described different paths for the two bicycles, a greater excursion was observed in the medio-lateral (y) axis (compared to the antero-posterior (x) and vertical (z), both for NB and RB. However the oscillation in forward direction seems to be smaller in NB compared to RB, in which we observed lower oscillation in the vertical axis. Volume calculated as the product of the three excursions showed no significant differences between bicycles and rpm (Table 6).

| NB | | | | |
|---|---|---|---|---|
| rpm | x (mm) | y (mm) | z (mm) | Vol (mm$^3$) |
| 50 | $8.0 \pm 2.9$ | $14.0 \pm 3.2$ | $10.0 \pm 0.6$* | $1177.2 \pm 694.7$ |
| 70 | $6.8 \pm 2.6$* | $15.0 \pm 3.9$ | $11.0 \pm 1.1$* | $1144.8 \pm 559.4$ |
| 90 | $5.2 \pm 1.3$* | $15.3 \pm 3.8$ | $12.1 \pm 1.4$ | $996.9 \pm 482.5$ |
| 110 | $5.9 \pm 0.7$ | $14.8 \pm 6.4$ | $13.4 \pm 2.7$ | $1221.2 \pm 826$ |
| *M* | $6.5 \pm 1.2$ | $14.8 \pm 0.5$ | $11.6 \pm 1.5$ | $1135.0 \pm 97.2$ |
| RB | | | | |
| rpm | x (mm) | y (mm) | z (mm) | Vol (mm$^3$) |
| 50 | $10.2 \pm 1.7$ | $10.7 \pm 7.1$ | $6.9 \pm 1.9$* | $830.5 \pm 782.7$ |
| 70 | $11.6 \pm 1.2$* | $15.6 \pm 5.4$ | $7.8 \pm 1.8$* | $1511.9 \pm 949.9$ |
| 90 | $9.0 \pm 1.5$* | $17.5 \pm 2.8$ | $10.3 \pm 2.4$ | $1651.3 \pm 653.5$ |
| 110 | $6.8 \pm 2.5$ | $16.8 \pm 4.0$ | $12.6 \pm 2.8$ | $1533.8 \pm 912.8$ |
| *M* | $9.4 \pm 2.0$ | $15.1 \pm 3.1$ | $9.4 \pm 2.6$ | $1381.9 \pm 372.6$ |

**Table 6**. BCoM excursion (in mm) in three axes and BCoM volume (in mm$^3$) on both bicycles $\pm$ *SD*. * indicates significant difference between bicycles ($p < 0.05$).

In figure 27 are presented Symmetry Indices in the three axis as mean ± standard deviation. The indices reached the highest value in the vertical axis (0.908 ± 0.046) for both bicycles. On the other directions we noticed a different trend for the two pedalling configurations. While for the NB the lowest values of symmetries regarded the antero-posterior direction, RB showed a minimum in the medio-lateral one. Statistical results also showed some differences between bicycles and rpm.
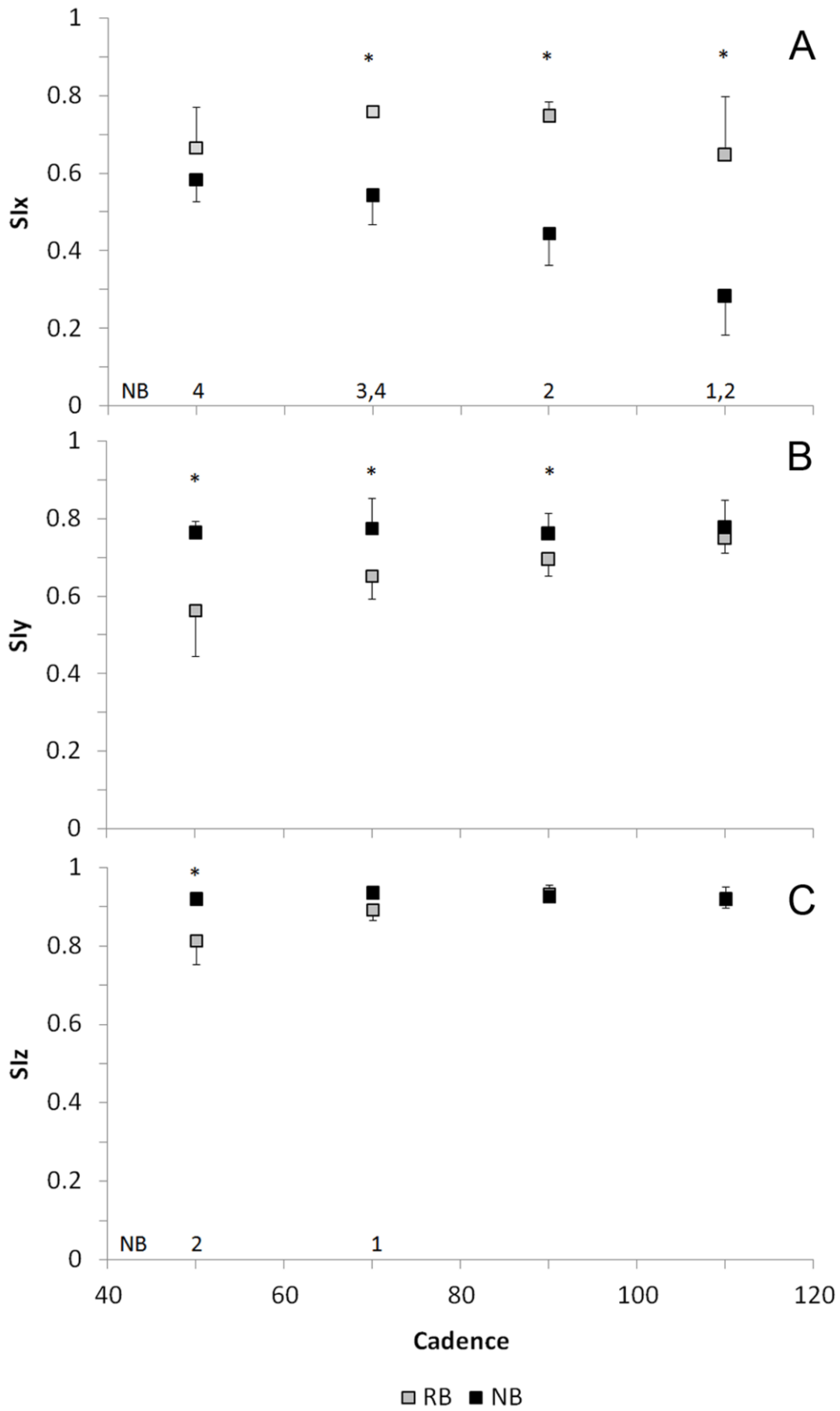
**Figure 27.** *SIx* (A),*SIy* (B) and *SIz* (C) at different rpm. Numbers 1,2,3,4 represent significant differences between 50,70,90,110 rpm respectively. * indicates difference between bicycles ($p < 0.05$).

In the following tables we reported the single Symmetry Indices SIx , SIy and SIz. Every subject has eight different indices, one for each pedalling frequency, for each axes. Statistical analysis showed that NB and RB

| SIx | NB | | | | RB | | | |
|---|---|---|---|---|---|---|---|---|
| Sogg | 50 | 70 | 90 | 110 | 50 | 70 | 90 | 110 |
| S1 | 0.544 | 0.608 | 0.536 | 0.329 | 0.737 | 0.767 | 0.728 | 0.635 |
| S2 | 0.612 | 0.478 | 0.351 | 0.232 | 0.666 | 0.774 | 0.754 | 0.785 |
| S3 | 0.533 | 0.482 | 0.412 | 0.177 | 0.747 | 0.752 | 0.800 | 0.730 |
| S4 | 0.653 | 0.608 | 0.487 | 0.399 | 0.519 | 0.753 | 0.712 | 0.445 |
| MEAN | 0.586 | 0.544 | 0.446 | 0.284 | 0.667 | 0.762 | 0.748 | 0.649 |
| SD | 0.057 | 0.074 | 0.081 | 0.099 | 0.105 | 0.011 | 0.038 | 0.149 |

| SIy | NB | | | | RB | | | |
|---|---|---|---|---|---|---|---|---|
| Sogg | 50 | 70 | 90 | 110 | 50 | 70 | 90 | 110 |
| S1 | 0.770 | 0.793 | 0.785 | 0.809 | 0.652 | 0.719 | 0.741 | 0.767 |
| S2 | 0.791 | 0.869 | 0.792 | 0.833 | 0.520 | 0.675 | 0.710 | 0.736 |
| S3 | 0.723 | 0.762 | 0.788 | 0.797 | 0.668 | 0.642 | 0.699 | 0.792 |
| S4 | 0.774 | 0.682 | 0.682 | 0.673 | 0.418 | 0.579 | 0.636 | 0.707 |
| MEAN | 0.765 | 0.776 | 0.762 | 0.778 | 0.565 | 0.654 | 0.696 | 0.750 |
| SD | 0.029 | 0.077 | 0.053 | 0.072 | 0.118 | 0.059 | 0.044 | 0.037 |

| SIz | NB | | | | RB | | | |
|---|---|---|---|---|---|---|---|---|
| Sogg | 50 | 70 | 90 | 110 | 50 | 70 | 90 | 110 |
| S1 | 0.916 | 0.926 | 0.928 | 0.882 | 0.744 | 0.861 | 0.944 | 0.906 |
| S2 | 0.929 | 0.944 | 0.947 | 0.955 | 0.892 | 0.924 | 0.918 | 0.895 |
| S3 | 0.924 | 0.946 | 0.948 | 0.936 | 0.808 | 0.880 | 0.931 | 0.937 |
| S4 | 0.907 | 0.923 | 0.887 | 0.906 | 0.815 | 0.908 | 0.941 | 0.940 |
| MEAN | 0.919 | 0.935 | 0.927 | 0.920 | 0.815 | 0.893 | 0.934 | 0.919 |
| SD | 0.010 | 0.012 | 0.029 | 0.032 | 0.061 | 0.028 | 0.011 | 0.022 |

**Table 7.** The symmetry indices along antero-posterior, medio-lateral and vertical axis (SIx, SIy, SIz respectively), derived from BCoM analysis during pedalling on NB and RB, for every subject and pedalling frequency. Also we reported the mean value and the SD for each rpm.

In the following two graphs we analysed differences between the symmetry indices in the three different directions, (SIx , SIy , SIz), for both bicycles. Results are presented as mean ± standard deviation (SD).



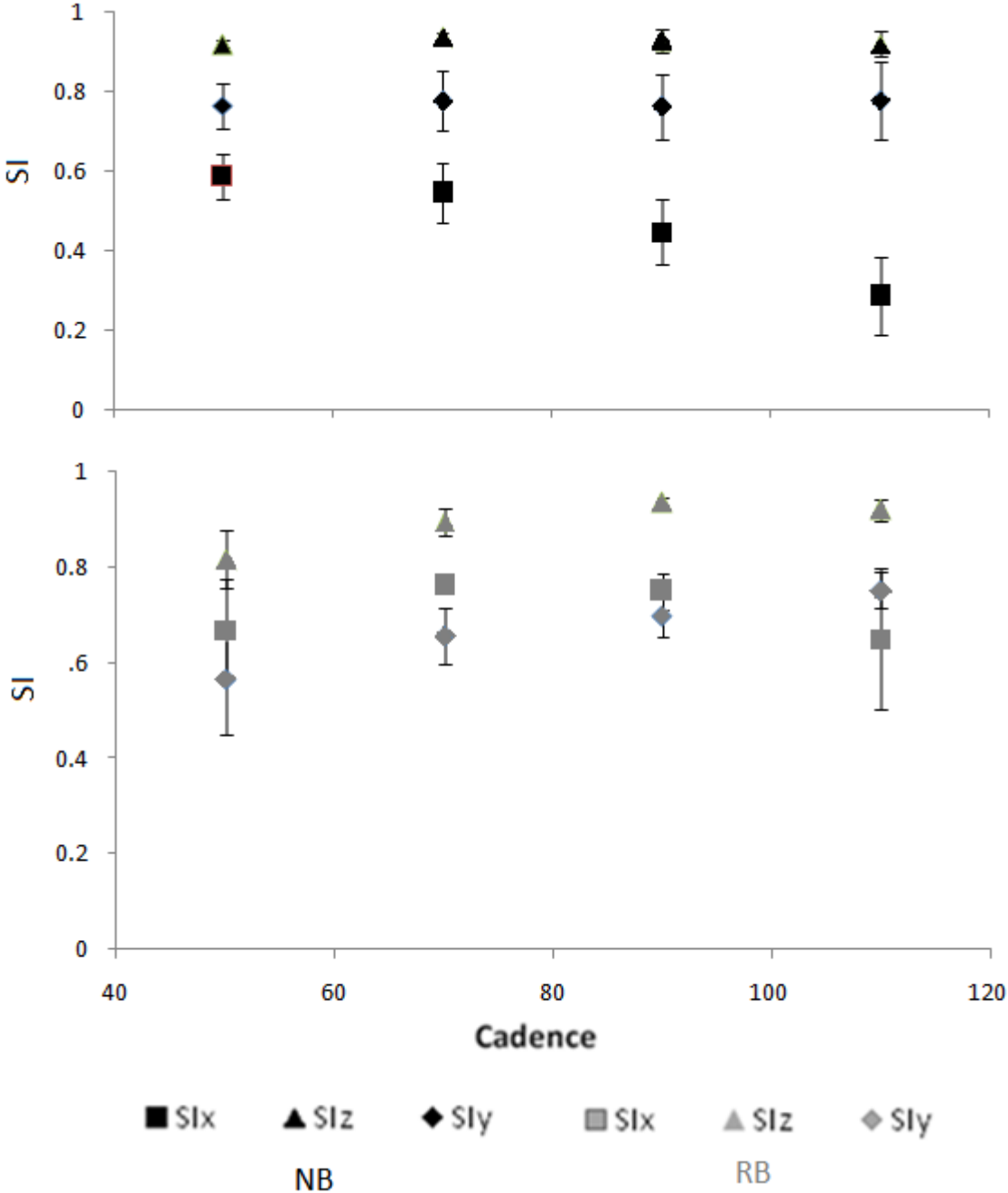**Figure 28.** SI in function of cadence for the three coordinates divided for the two kinds of bicycle, normal and recumbent.

## 3.4 Mechanical work

As assumed $\dot{W}_{EXT}$ measured by the SRM for the same target pedalling frequency (RPM) could be considered constant, maintaining similar values for the two bicycles with a difference always lower than 5% between them (table 8). We have also reported the real pedalling frequency (rpm) measured by the instrument.

| BICYCLE | RPM | rpm | | $\dot{W}_{EXT}$ | |
|---------|-----|------|-----|------|-----|
| | | mean | SD | mean | SD |
| NB | 50 | 50 | 1.1 | 37 | 1.7 |
| NB | 70 | 70 | 0.8 | 60 | 2.1 |
| NB | 90 | 90 | 0.3 | 81 | 4.2 |
| NB | 110 | 110 | 1.4 | 109 | 8.4 |
| RB | 50 | 50 | 0.2 | 39 | 1.5 |
| RB | 70 | 69 | 1.2 | 57 | 2.5 |
| RB | 90 | 89 | 1.3 | 79 | 5.6 |
| RB | 110 | 109 | 3.1 | 104 | 7.2 |

**Table 8.** Real pedalling frequency (rpm) and mechanical external power ( $\dot{W}_{EXT}$ ) at different target RPM for both bicycles.

The mechanical internal work rate has been modeled for bipeds by Minetti and Saibene (1992), and then extended to quadrupeds (Minetti, 1998) and, more recently, for bicycling (Minetti et al., 2001). In our study the mechanical internal work rate, or internal power, ranged from 7.90 W to 65.15 W in NB and from 7.25 W to 62.16 W in RB, increasing as function of the rpm, with the following regression equation:

$$W_{INT} = k * m * fr^{3}$$

where *k* had a value of 0.176 and 0.161 respectively for RB and NB, *m* was the mass of a subject in kg and *fr* was the pedalling frequency in Hz. No significant difference was found between bicycles; likewise values obtained from the WM simulation were the same in upright (NBWM) and recumbent (RBWM) posture (Figure 29A).

The additional external mechanical power was always higher in NB compared to RB in both real and simulated pedalling task, although we found significant differences between bicycles in real condition only at specific cadences (Figure 29B).
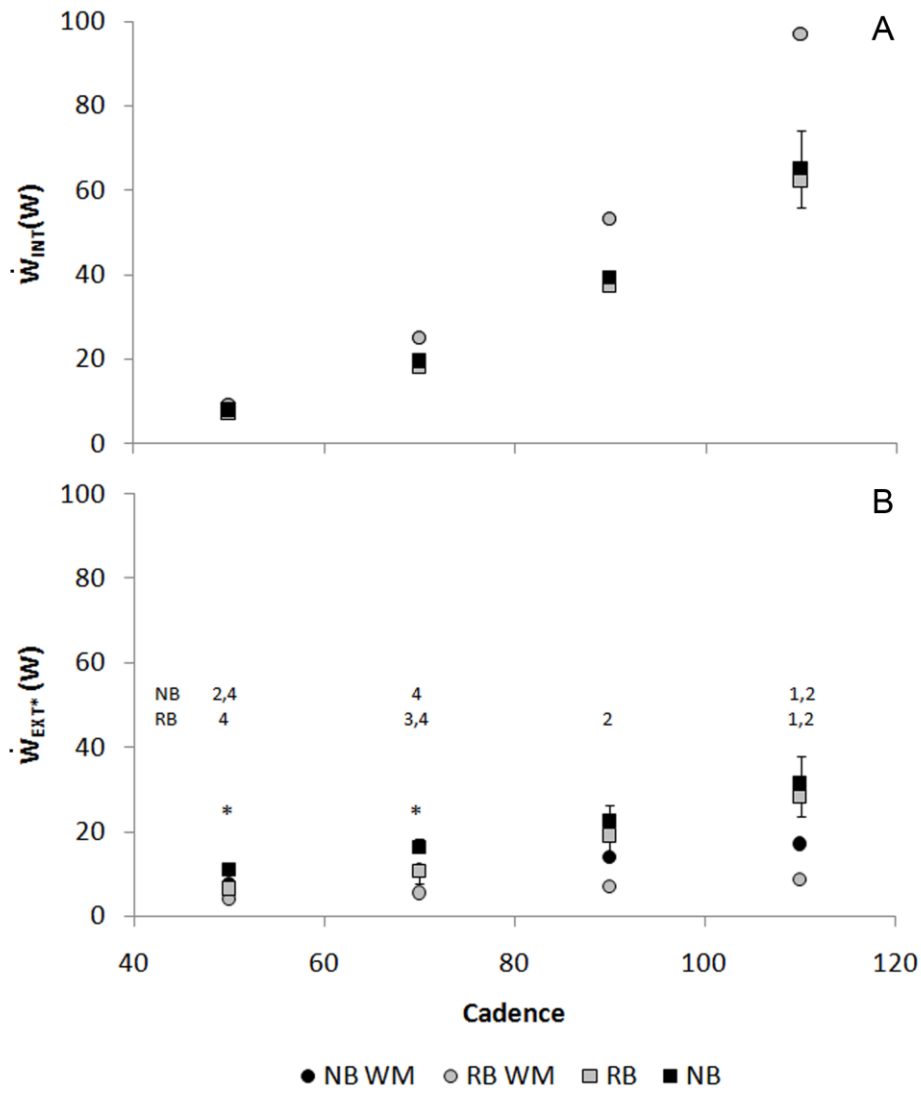
**Figure 29.** Mechanical internal (A) and additional external (B) power as function of rpm in both real (NB and RB) and simulated (NB WM, RB WM) pedalling task. Numbers 1,2,3,4 indicate significant differences between 50,70,90,110 rpm respectively. * indicates significant difference between bicycles ($p < 0.05$).

# CHAPTER FOUR

# Discussion

The purpose of our study was to compare NB and RB through the investigation of the non-aerodynamic factors affecting performance on both bicycles: MTL changes, BCoM trajectories and its symmetries and mechanical work rate. In addition to the comparison between the two bikes the effect of pedaling frequency was also analyzed.

## 4.1 Joint Angle and Muscle-Tendon Length

With the hypothesis that the change in posture alters joint angle, we analyzed this variable by comparing the two bicycles at different rpm. Sanderson et al. (2006) reported that, in a group of competitive cyclists, the range of motion at the knee decreases when pedalling cadence increases (an increase of 4° from 50 to 110 rpm), while the change in the range of motion at the ankle joint was higher (an increase of 10° from 50 to 110 rpm). In contrast to that work, we not found any difference due to the pedalling frequency. Our study evaluated recreational and not competitive cyclist. Joint angles vary between subjects due to anthropometry and pedalling technique but also may vary between the legs of a single subject due to anatomical asymmetry of the two legs and to asymmetry in pedalling mechanics (Lafortune et al., 1983). Skill level of the cyclist, anatomical differences and pedalling technique could be the reasons why no differences in joint angle at different rpm were founded in this work.

Technical data and the position of the riders on the bicycles were reported in method section in order to give a general overview of the different posture when using a normal or recumbent bicycle. Hip and Knee angles are the included angles between the pelvis and the thigh and thigh and shank respectively when the joint is flexed. A full joint extension corresponds to 180° for both joints (i.e. when the subject is standing). The ankle angle is included between the shank and the foot. The paired T test highlights that different configuration due to the different bicycles cause changes in joint angle when riding the two bicycles. The comparison of hip, knee and ankle angles in NB and RB, which are plotted in

function of crank angle in figure 24, highlights the differences of these joints. By calculating the average angle (the mean between all maximum and minimum angles reached during the pedalling cycle at different rpm) it results that hip, knee and ankle are more extended in RB (+6° on average).

In addition to the analysis of these three joints, we also evaluated the movements of the trunk during the pedal cycle. It is interesting to note that, when left hip joint extends, the trunk leans sideways to the right and vice versa (figure 30).
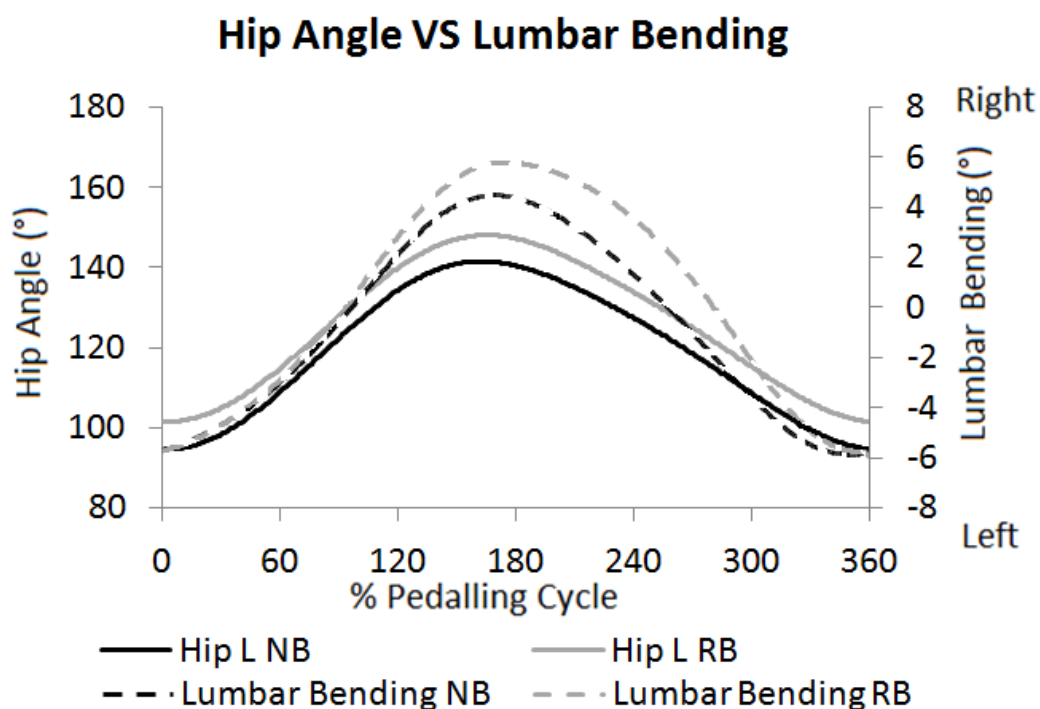


**Figure 30.** Joint angle (°) of the left hip and lumbar bending over a complete crank cycle. Positive values of lumbar bending indicate that the trunk is tilted to the right, negative values indicate that the trunk is tilted to the left.

The kinematics analysis of the joint angles was the starting point for the analysis of the muscle-tendon length changes in both configurations, which was one of the aims of this thesis. Indeed, even if ultrasound can be considered an important tool for the analysis of in vivo skeletal muscle architecture in static and dynamic condition, it difficult to use in fast movement. For this reason kinematical data collected during pedalling were utilized also to estimate the effect of posture on muscle tendon length changes. Muscle-tendon kinematic was here obtained via a biomechanical model in conjunction with experimental data which

quantify both the position and orientations of body segments during the activity of interest. This allowed us to investigate the hypothesis that one of the two pedalling positions could be more advantageous than the other because of the range of contraction of different muscle-tendon units. It is know that cycling is an activity that involves different muscles: hip extensors and flexors, knee extensor and flexors, ankle plantar-flexors and dorsi-flexors. However the muscles involved in the pedalling task cannot be classified as propulsive or not: i.e. the Biceps Femoris is typically a knee flexor (movement that characterizes the recovery phase), but in cycling is active also during the hip extension (typical of the propulsive phase). Similar considerations can be made for the Rectus Femoris.

Since human vastus lateralis, a major knee extensor muscle (Narici et al 1989), works in the plateau and descending limb of the force-length relationship during cycling (Austin et al., 2010; Muraoka et al., 2001) and this muscle was more shortened in RB in our simulation, it probably operates nearer its optimal length in RB than NB. For this reason we can speculate that recumbent riders take advantage of the plateau region of the Vastus Lateralis force-length relationship, thus cycling in RB is better from a force-length perspective of this muscle. Differently, during upright cycling, medial and lateral gastrocnemius work only in the ascending part (Maganaris, 2003), while tibialis anterior and soleus in the ascending and plateau region too (Maganaris, 2001). Our results showed that soleus (+1.6%), Lateral (+0.9%) and medial gastrocnemius (+0.9%) are, on average, more elongated in the normal bicycle, while tibialis antirior is more stretched (+1.9) when pedalling in RB. Comparing our data with literature we can speculate that the firsts three muscles are in a better range of their force-length relationships in NB while the tibialis antirior is advantaged in RB. Unfortunately, data regarding the force-length relationship during cycling in the other muscles reported in Table 4 and 5 are not present in literature and we do not know if they are working in a portion closer or farther to their optimal length. Although we estimated the MTL (the distance between bone insertions of a muscle), this is not enough to simulate the muscle force-length behaviour and force velocity-properties, but this analysis could be the starting point for further investigations. Indeed, differently from the MTL estimation that need only kinematic data (Riley et al., 2010), muscle fibre length could be investigated with a forward dynamic analysis (Thelen et al., 2005; Chumanov, Heiderscheit & Thelen, 2007; Zajac, 1989), focusing the attention on the most important muscles of cycling.

## 4.2 Body Centre of Mass analysis

Our experimental data confirmed that BCoM contour described a trajectory similar to an ellipse in the sagittal plane (figure 26C), similarly to a simulation of pedalling lower limbs (Minetti, 2011) with differences in the major axis inclination between the two bicycles. It was more perpendicular to the ground in NB compared to RB and this could explain the difference of excursions on x and z axes.

In this study, the comparison between the two bicycles shows that the BCoM moved inside a cube with a side length smaller than 15 mm without significant differences in the two bicycles. Indeed the excursion of BCoM was greater in the progression axis in RB compared to NB while lower in the vertical one and, consequently, the volume occupied was not different (Table 6). In the frontal plane the BCoM trajectory was in the form of a "U" in NB (figure 26D) and of an inverted "U" in RB (figure 26E); while in the transverse one a figure of "8" was drawn in both bicycles. This means that the trajectory of BCoM is smaller when compared to human walking, where it has been widely demonstrated that it moves within a cube of 40 mm side (Whittle, 1977).

Despite the fact that the excursion of the centre of mass seemed to increase with pedalling frequency, no significant difference were found increasing rpm both for NB and RB (Table 1).

Comparing the real BCOM paths obtained during experimental sessions with the 2D BCoM trajectories from WM simulation (figure 26), some similarities could be detected and differences between them can be attributed to the slight discrepancy in body segments length and to the small motion of the trunk. Looking at figure 25B, when one of the two shanks in WM simulation was shortened replicating a physiological and common anatomical asymmetry between limbs, the BCoM trajectories become similar to the experimental one (figure 26C), underling the hypothesis that anatomical asymmetry may cause dynamical and spatial asymmetry of the BCoM in locomotion (Gurney et al., 2001; Seeley et al., 2010; Seminati et al., 2013).

Starting from the BCoM trajectory, its dynamical symmetries have been evaluated previously in different gaits and species (Biancardi et al., 2011; Minetti et al., 2011; Seminati et al., 2013) but never in human cycling. Our data showed that the highest symmetries were reached in the vertical axis in both bicycles probably because the saddle could limit the movements along it. In the antero-posterior axis the RB showed higher symmetry values,

compared to NB, and this can be attributed to the backrest that stabilize the trunk and inhibit its movement in the progression axis. In NB, differently from RB, SIx was significantly lower decreasing with increasing rpm while in the medio-lateral axis the symmetry was not affected by the pedalling frequencies, showing SIy values always higher compared to RB. In both bicycles there are no constrain limiting the movements in the frontal plane, and this is more evident in the RB at low rpm, probably due to the fact that each subject was more accustomed with cycling on NB and less on RB. Skilled and trained cyclists could be more symmetrical than our untrained subjects, for this reasons further analysis should be done by comparing experienced riders on RB and NB, in order to understand which bicycle allows to reach higher dynamical symmetry and if the level of training could have effects on the level of symmetry and, possibly, to cycling economy.

## 4.3 Mechanical work

Moreover, the BCoM analysis allowed us to investigate the components of the total mechanical work necessary to sustain the pedalling task.

It is reported that total mechanical work in cycling is partitioned into the work of the vehicle with respect to the external environment and the one related to the propelling machinery. The first includes the work to overcome air drag and rolling resistance which makes what is known as the mechanical external work that we have kept constant and monitored through an SRM (table 8). The work related to propelling machinery has two principal components: the additional mechanical external work due to a small residual movement of the body centre of mass and the mechanical internal work. We focalized on this two aspect of work that have never before been analyzed on RB. The internal work has to be considered when riding a bicycle (Francescato et al., 1995) because it is well known that, for the same external power output ($\dot{W}_{EXT}$), an increasing in rpm is associated to an increment of oxygen consumption due to a larger mechanical internal work (Coast et al., 1986). More recently, this metabolic equivalent of the 'kinetic' internal work has been questioned since the WM simulation of pedalling showed that the pedals rotation could occur indefinitely with no need of power input (Minetti, 2011), suggesting that the measurable (but negligible) 'kinetic' internal work could be proportional to the not-measurable 'viscous' internal one, that could be the real responsible of the VO2 increment due to high pedalling rate. The internal work

rate was related principally to the pedalling frequency (figure 29A) with no differences between NB and RB. In addition, our analysis showed that the internal power, depending on the 3rd power of pedalling frequency in Hz, have similar value for RB: indeed the relation between cadence and $\dot{W}_{INT}$ in RB was in line with previously results (figure 31). Moreover, our data are in line with Francescato and collaborators (1995) that have quantified $\dot{W}_{INT}$ through a metabolic approach, which was related to lower limb mass and pedalling frequency. Indeed they have found amounts of 6, 28 and 86 W when frequency pedalling increased to 61, 88 and 115 RPM respectively.
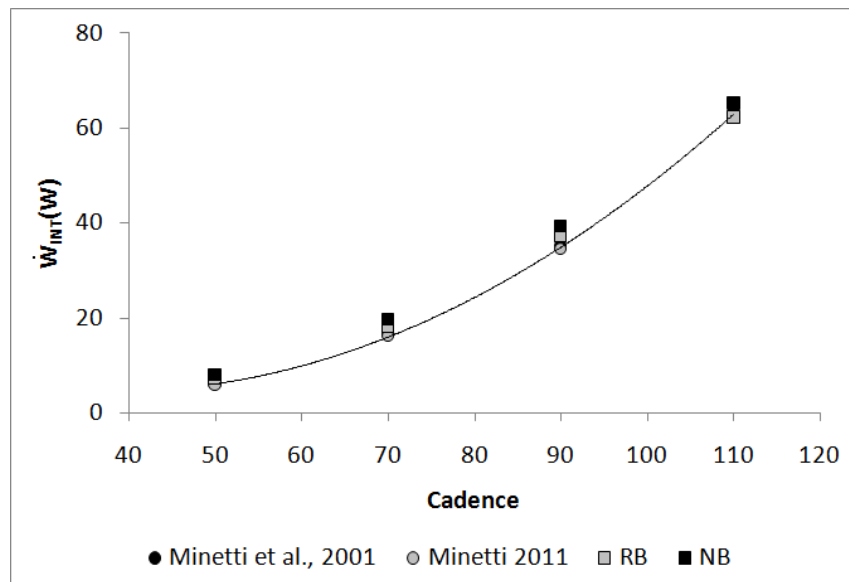


**Figure 31.** Values of internal power of each of our subjects as function of rpm while riding a NB (k= 0.176), RB (k= 0.161) and data from Minetti et al., 2001 (k= 0.153) and Minetti 2011 (k=0.150). Values of k were calculated with the pedalling frequency in hz.

In addition the recent observations of Minetti (2011) regarding the possible contribution of an supplementary component in the mechanical external power, led us to consider also the additional mechanical external power ($\dot{W}_{EXT*}$) necessary to lift and accelerate the BCoM even when the bicycle is stationary placed on rolls. Differences in cycling position affected only the potential energy associated to the BCoM and not the kinetic one, with effects on the total energy and on the additional mechanical external work $W_{EXT*}$. Both in experimental session and in WM simulation $\dot{W}_{EXT*}$ was found to be greater in NB than RB for

all cadences (Figure 29B) probably due to the changed orientation of BCoM profile while riding the two bicycles. Other differences in the additional external work could be due to the fact that, differently from the general belief that the BCoM travels parallel to the ground during bicycling on the sagittal plane, in our experimental sessions it moved along all three spatial axes, especially in the medio-lateral one (Table 6). This excursion on the y axis could be associated to the lumbar bending analyzed and reported in figure 30: despite a relatively small movement of the trunk of about 10°, this could significantly affect the trajectory of the body center of mass.

In this work the external power increases with pedalling frequency due to the fact that the external force (represented by rolling resistance) was maintained constant (table 8). In absolute terms the contribution of $\dot{W}_{EXT*}$ to the total mechanical power is not negligible, ranging from 11 to 31 W in NB and from 6 to 29 in RB. in this work). Also the relative contribution of $\dot{W}_{EXT*}$ to the total mechanical power is always lower in RB when compared to NB (see figure 32) and this difference could be responsible for differences in mechanical efficiency (but not evaluated in this thesis). It is thought that the 3D trajectory of body centre of mass could determine an increase of the total mechanical work, and as a consequence, the metabolic one could be greater as well. In order to improve cycling locomotion in term of metabolic cost, $\dot{W}_{EXT*}$ should be limited, avoiding an excessive excursion of BCoM.
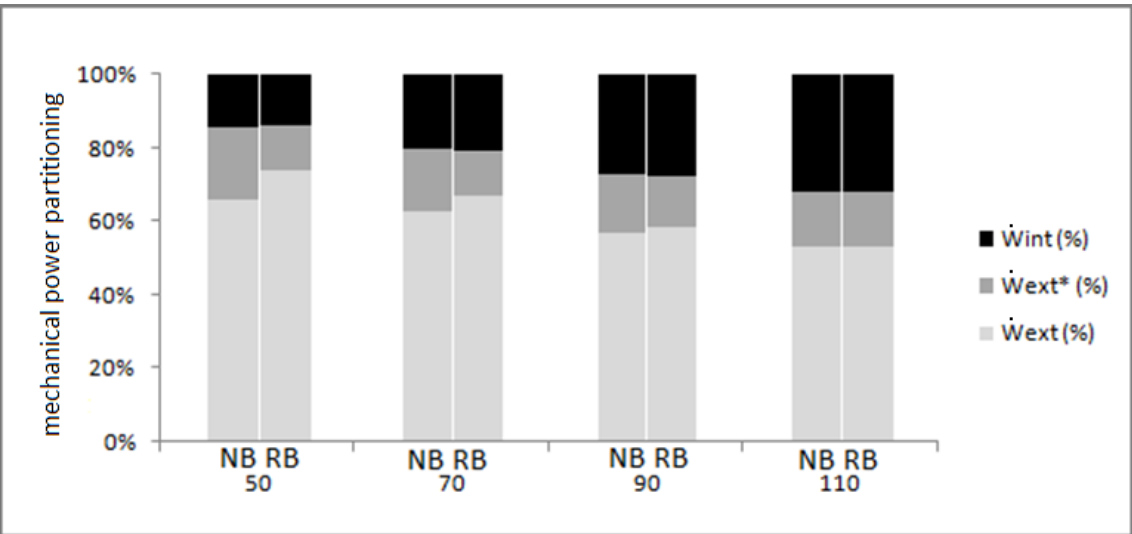


**Figure 32.** Mechanical work partitioning for each pedalling cadence in normal (NB) and recumbent (RB) bicycle.

# CHAPTER FIVE

# Conclusion

## 5.1 Limits and further perspective

Some limitations of the present study and further perspective need to be addressed.

The seat to pedal distance has been carefully measured, but the lack of a saddle which prevents the movement of the pelvis (toward or away from the pedals) may cause in RB slight variations in this parameter, with impact on joints range of motion and muscle tendon length changes.

Additionally, the muscle tendon length changes have been analyzed in this work, but to better understand muscle function during cycling in terms of the force–length and force–velocity properties, it should be better to characterize the lengths of muscle fibres relative to their optimal length. However, it is difficult to direct measure the operating length of muscle fibres during complex and fast movement. Indeed their determination requires medical imaging of sarcomere length, i.e. laser diffraction or ultrasound measurement but these techniques are difficult to achieve on a bicycle. The use of a recent musculoskeletal model (Arnold et al., 2010), together with the force signal derived from force sensor applied to the pedals, could be useful to develop a dynamical simulation of pedalling cyclist with OpenSim, in order to calculate the fibre operative lengths of human lower limb muscles during cycling. With this method, differences in fibre lengths could be better understood, highlighting on which limbs of the force–length curve (ascending limb, descending limb and plateau) do lower limb muscles operate during the pedalling cycle.

Moreover, the small sample size can influence the statistical significance of some variables due to the fact that changes that may be occurring can be deleted by variability between subjects when the pedalling position is altered. By increasing the number of subjects and comparing professional (skilled in pedalling on NB and RB) and recreational cyclists could be a useful way to better analyze the trajectory of BCoM and its features in order to mathematically describe kinematic variables related to the BCOM in both categories of

riders. In this way variations could be detected in locomotion dynamics such as those caused by training.

A previous study reported that, while no correlations were found between anatomical and kinematic variables and the metabolic cost of transport in human running, the most trained subjects showed the highest level of kinematic symmetry during running (Seminati et al. 2013). Since a certain level of asymmetry during cycling has been reported, it would be interesting to study its effect in terms of energy cost.

## 5.2 Conclusion

In the introduction of this thesis the characteristics of the recumbent bicycle have been analized highlighting the differences and analogies with NB. Our aim was to investigate the differences between the two pedalling positions that were not been studied yet. Results of this study confirm experimentally, for the first time, the existence of a 3D BCoM movement with its associated additional mechanical external work, previously evaluated only with a physical cycling simulation. The comparison of the two bicycles showed that the BCoM changed its orientation but maintained a similar pattern in both configurations, with consequently advantages for the RB: a smaller $\dot{W}_{EXT*}$ and a greater Symmetry Index on the progression axis. However, although the results reported that muscles were working at slightly different operative ranges of their length, the final propulsive effectiveness is difficult to assess, because the differences never exceeded the 4% of resting length. Looking at these bicycles from a kinematical perspective we could speculate that the RB position can be partially considered a 90° backward rotated NB. Therefore we could conclude that only small differences are appreciable between the two bicycles, and the principal benefit due to ride a RB still remains the aerodynamic factor. Suggestion that could be inferred from this work regards the development of mechanisms reducing the energy expenditure related to the $\dot{W}_{EXT*}$ and increasing the stability of the bicycle.

**References**

1. Alexander, R. M. (2003). Principles of Animal Locomotion. Published by Princerton University Press, 41 William Street, Princerton, New Jersey.
2. Ardigo`, L.P., Goosey-Tolfrey, V.L., and Minetti, A.E., 2005. Biomechanics and energetics of basketball wheelchairs evolution. International Journal of Sports Medicine, 26, 388–396.
3. Ashe, M. C., Scroop, G. C., Frisken, P. I., Amery, C. A., Wilkins, M. A., & Khan, K. M.(2003). Body position affects performance in untrained cyclists. British Journal of Sports Medicine, 37(5), 441–444
4. Austin, N., Nilwik, R., Herzog, W. (2010). In vivo operational fascicle lengths of vastus lateralis during sub-maximal and maximal cycling. Journal of Biomechanics, 43, 2394–2399.
5. Baum, B. S., & Li, L. (2003). Lower extremity muscle activities during cycling are influenced by load and frequency. Journal of Electromyography and Kinesiology, 13(2), 181-190.
6. Biancardi, C. M., Fabrica, C. G., Polero, P., Loss, J. F., & Minetti, A. E. (2011). Biomechanics of octopedal locomotion: kinematic and kinetic analysis of the spider Grammostola mollicoma. The Journal of Experimental Biology, 214(20), 3433-3442.
7. Bisi MC, Ceccarelli M, Riva F, Stagni R.( 2012) Biomechanical and metabolic responses to seat-tube angle variation during cycling in tri-athletes." Journal of Electromyography and Kinesiology Dec;22(6):845-51
8. Brown, D. A., Kautz, S. A., & Dairaghi, C. A. (1996). Muscle activity patterns altered during pedaling at different body orientations. Journal of Biomechanics, 29, 1349–1356.
9. Burke, E. R., & Pruitt, A. L. (2003). Body positioning for cycling. In E. R.Burke (Ed.), High-tech cycling2nd ed. (pp. 69–92). Champaign: HumanKinetics
10. Capelli, C., Ardigo, L. P., Schena, F., & Zamparo, P. (2008). Energy cost and mechanical efficiency of riding a human-powered recumbent bicycle. Ergonomics, 51(10), 1565-1575.
11. Cavagna GA, Franzetti P (1986) The determinants of the step frequency in walking in humans. J Physiol 373:235–242
12. Cavagna G.A., Saibene F., Margaria R. (1964) Mechanical work in running. J. Appl. Physiol. 19: 249-256.
13. Cavagna G.A., Thys H., Zamboni A. (1976) The sources of external work in level walking and running. J. Physiol. 262: 639-657.
14. Cavagna, G. A., & Kaneko, M. (1977). Mechanical work and efficiency in level walking and running. The Journal of Physiology, 268(2), 467-481.
15. Chumanov, E. S., Heiderscheit, B. C., & Thelen, D. G. (2007).The effect of speed and influence of individual muscles on hamstring mechanics during the swing phase of sprinting. Journal of Biomechanics, 40(16), 3555-3562.
16. Coast, J. R., Cox, R. H., & Welch, H. G. (1986). Optimal pedalling rate in prolonged bouts of cycle ergometry. Medicine and Science in Sports and Exercise, 18(2), 225-230.
17. Convertino, V. A., Goldwater, D. J., & Sandler, H. (1984). Oxygen uptake kinetics of constant-load work: upright vs. supine exercise. Aviation, Space, and Environmental Medicine, 55(6), 501-506.
18. Davis III, R. B., Ounpuu, S., Tyburski, D., & Gage, J. R. (1991). A gait analysis data collection and reduction technique. Human Movement Science, 10(5), 575-587.
19. Diaz FJ, Hagan RD, Wright JE, Horvath SM (1978) Med Sci Sports. Fall;10(3):214-7. Maximal and submaximal exercise in different positions.
20. Delp, S. L., Anderson, F. C., Arnold, A. S., Loan, P., Habib, A., John, C. T., & Thelen, D. G. (2007). OpenSim: open-source software to create and analyze dynamic simulations of movement. IEEE Transactions on Biomedical Engineering, 54(11), 1940-1950.

21. di Prampero, P. E. (2000). Cycling on Earth, in space, on the Moon. European journal of applied physiology, 82(5-6), 345-360.

22. di Prampero PE (1986) The energy cost of human locomotion on land and in water. Int J Sports Med. 7: 55-72

23. di Prampero PE, Cortili G, Mognoni P, Saibene F (1979) Equation ofmotion of a cyclist. J Appl Physiol 47(1):201–206

24. Egana, M., Columb, D., & O'Donnell S. (2013). Effect of low recumbent angle on cycling performance, fatigue, and VO2 kinetics. Medicine & Science in Sports & Exercise, 45(4), 663-673.

25. Egana, M., O'Riordan, D., & Warmington, S. A. (2010). Exercise performance and VO2 kinetics during upright and recumbent high-intensity cycling exercise. European Journal of Applied Physiology, 110(1), 39-47.

26. Egana, M., & Green, S. (2005). Effect of body tilt on calf muscle performance and blood flow in humans. Journal of Applied Physiology, 98(6), 2249-2258.

27. Egana, M., Green, S., Garrigan, E. J., & Warmington, S. (2006). Effect of posture on high-intensity constant-load cycling performance in men and women. European Journal of Applied Physiology, 96(1), 1-9.

28. Eiken, O. (1988). Effects of increased muscle perfusion pressure on responses to dynamic leg exercise in man. European Journal of Applied Physiology and Occupational Physiology, 57(6), 772-776.

29. Eisner, W. D., Bode, S. D., Nyland, J., & Caborn, D. N. M. (1999). Electromyographic timing analysis of forward and backward cycling. Medicine and Science in Sports and Exercise, 31, 449–455.

30. Elftman, H. (1939). The force exerted by the ground in walking. Arbeitsphysiologie, 10, 485–491.

31. Evangelisti, M. I., Verde, T. J., Andres, F. F., & Flynn, M. G. (1995). Effects of handlebar position on physiological responses to prolonged cycling. Journal of Strength & Conditioning Research, 9(4), 243–246

32. Faria, E. W., Parker, D. L., & Faria, I. E. (2005). The science of cycling: factors affecting performance–part 2. Sports Medicine, 35(4), 313-337.

33. Fenn, W. O. (1930). Frictional and kinetic factors in the work of sprint running. American Journal of Physiology--Legacy Content, 92(3), 583-611.

34. Ferrer-Roca, V., Bescós, R., Roig, A., Galilea, P., Valero, O., & García-López, J. (2014). Acute effects of small changes in bicycle saddle height on gross efficiency and lower limb kinematics. The Journal of Strength & Conditioning Research, 28(3), 784-791.

35. Formenti F, Minetti AE. (2007). Human locomotion on ice: the evolution of ice-skating energetics through history.  J Exp Biol. England, 1825-1833.

36. Formenti, F., Ardigò, L. P., & Minetti, A. E. (2005). Human locomotion on snow: determinants of economy and speed of skiing across the ages. Proceedings of the Royal Society B: Biological Sciences, 272(1572), 1561-1569.

37. Francescato, M. P., Girardis, M., & Di Prampero, P. E. (1995). Oxygen cost of internal work during cycling. European Journal of Applied Physiology and Occupational Physiology, 72(1-2), 51-57.

38. Gregor, R. J., & Conconi, F. (2000). Anatomy, biochemistry and physiology of road cycling. In R. J. Gregor, & F. Conconi (Eds.), Road Cycling (pp. 1–17). Oxford: Blackwell Science.

39. Gregor, R. J., Broker, J. P., & Ryan, M. M. (1991). The biomechanics of cycling. Exercise and Sport Sciences Reviews, 19, 127–169.

40. Gross A. C., Kyle C. R., Malewicki D. J. (1983). The aerodynamics of human-powered land vehicles. Sci Am; 249: 142-52

41. Gurney, B., Mermier, C., Robergs, R., Gibson, A., & Rivero, D. (2001). Effects of limb-length discrepancy on gait economy and lower-extremity muscle activity in older adults. The Journal of Bone & Joint Surgery, 83(6), 907-915.

42. Hakansson, N. A., & Hull, M. L. (2005). Functional roles of the leg muscles when pedaling in the recumbent versus the upright position. *Journal of biomechanical engineering*, *127*(2), 301-310.

43. Hamley EJ, Thomas V. 1967 Physiological and postural factors in the calibration of the bicycle ergometer. J Physiol. Jul;191(2):55P-56P

44. Hamner, S. R., Seth, A., & Delp, S. L. (2010). Muscle contributions to propulsion and support during running. Journal of biomechanics, 43(14), 2709-2716

45. Heil DP, Wilcox AR, Quinn CM (1995) Cardiorespiratory responses to seat-tube angle variation during steady-state cycling.. Med Sci Sports Exerc. May;27(5):730-5

46. Hill, A. V. (1938). The heat of shortening and the dynamic constants of muscle. Proc. R. Soc. B, 126, 136-195.

47. Hogberg P (1952) How do stride length and stride frequency influence the energy-output during running? Arbeitsphysiologie 14:437–441

48. Hubenig, L. R., Game, A. B., Kennedy, M. D. (2011). Effect of Different Bicycle Body Positions on Power Output in Aerobically Trained Females. Research in Sports Medicine, 19:245–258,

49. Hughson RL, Xing HC, Borkhoff C, Butler GC. Kinetics of ventilation and gas exchange during supine and upright cycle exercise. Eur J Appl Physiol Occup Physiol. 1991;63(3-4):300–7

50. Hull M. L., Hawkins D. A. (1990). Analysis of muscular work in multisegmental movements: application to cycling  J. Winters, S.-Y. Woo (Eds.), Multiple Muscle Systems, Springer, New York pp. 621–638

51. Inbar O, Dotan R, Trousil T, Dvir Z (1983) The effect of bycicle crank-length variation upon power performance. Ergonomics 26:1139-1146

52. Kautz S.A., Neptune R.R. (2002) Biomechanical determinants of pedaling energetics: internal and external work are not independent. Exerc. Sport Sci. Rev. 30 (4): 159-165.

53. Kadaba, M. P., Ramakrishnan, H. K., & Wootten, M. E. (1990). Measurement of lower extremity kinematics during level walking. Journal of Orthopaedic Research, 8(3), 383-392.

54. Kaneko M, Matsumoto M, Ito A, Fuchimoto T (1987) Optimum step frequency in constant speed running. In: Jonsson B (ed) Biomechanics X-B vol. 6B. Human Kinetics Publishers, Champaign, pp 803–807

55. Koga, S., Shiojiri, T., Shibasaki, M., Kondo, N., Fukuba, Y., & Barstow, T. J. (1999). Kinetics of oxygen uptake during supine and upright heavy exercise. Journal of Applied Physiology, 87(1), 253-260.

56. Leyk, D., Eßfeld, D., Hoffmann, U., Wunderlich, H. G., Baum, K., & Stegemann, J. (1994). Postural effect on cardiac output, oxygen uptake and lactate during cycle exercise of varying intensity. European Journal of Applied Physiology and Occupational Physiology, 68(1), 30-35.

57. Liu, M. Q., Anderson, F. C., Schwartz, M. H., & Delp, S. L. (2008). Muscle contributions to support and progression over a range of walking speeds. Journal of biomechanics, 41(15), 3243-3252.

58. Maganaris, C. N. (2001). Force–length characteristics of in vivo human skeletal muscle. Acta Physiologica Scandinavica, 172(4), 279-285.

59. Maganaris, C. N. (2003). Force-length characteristics of the in vivo human gastrocnemius muscle. Clinical Anatomy, 16(3), 215-223.

60. Margaria R. Sulla fisiologia e specialmente sul consumo energetico, della marcia e della corsa a varie velocità ed inclinazioni del terreno. Atti Acc Naz Lincei. 1938: 7: 299-368.

61. J.C. Martin  W.W. Spirduso  Determinants of maximal cycling power: rank length, pedaling rate and pedal speed Eur J Appl Physiol (2001) 84; 413-418

62. Minetti, A. E. and Ardigò, L. P. (2002). Halteres used in ancient Olympic long jump. Nature 420, 14-15.

63. Minetti, A. E., Ardigo, L. P., & Saibene, F. (1993). Mechanical determinants of gradient walking energetics in man. The Journal of Physiology, 472(1), 725-735.

64. Minetti, A. E. (1998). A model equation for the prediction of mechanical internal work of terrestrial locomotion. Journal of Biomechanics, 31(5), 463-468.

65. Minetti, A. E. (2011). Bioenergetics and biomechanics of cycling: the role of 'internal work'. European Journal of Applied Physiology, 111(3), 323-329.

66. Minetti, A. E., Cisotti, C., & Mian, O. S. (2011). The mathematical description of the body centre of mass 3D path in human and animal locomotion. Journal of Biomechanics, 44(8), 1471-1477.

67. Minetti, A. E., Pavei, G., & Biancardi, C. M. (2012).The energetics and mechanics of level and gradient skipping: Preliminary results for a potential gait of choice in low gravity environments. Planetary and Space Science, 74(1), 142-145.

68. Minetti, A. E., Pinkerton, J., & Zamparo, P. (2001). From bipedalism to bicyclism: evolution in energetics and biomechanics of historic bicycles. Proceedings of the Royal Society of London. Series B: Biological Sciences, 268(1474), 1351-1360.

69. Minetti A.E., Saibene F. (1992) Mechanical work rate minimization and freely chosen stride frequency of human walking: a mathematical model. J. Exp. Biol. 170: 19-34

70. Minetti A.E., Ardigò L.P., Saibene F. (1993) Mechanicals determinants of gradient walking energetics in man. J. Physiol. 471: 725-735

71. Morgan D, Martin P, Craib M, Caruso C, Clifton R, Hopewell R (1994) Effect of step length optimization on the aerobic demand of running. J Appl Physiol 77:245–251

72. Muraoka, T., Kawakami, Y., Tachi, M., & Fukunaga, T. (2001). Muscle fiber and tendon length changes in the human vastus lateralis during slow pedaling. Journal of Applied Physiology, 91(5), 2035-2040.

73. Nardello F., Ardigo` L. P., Minetti A. E. (2009). Human locomotion: Right/left symmetry in 3D trajectory of body centre of mass. *Gait & Posture* 30(S):S802S81

74. Neptune, R.R., Kautz, S.A., & Hull, M.L. (1997). The effect of pedaling rate on coordination in cycling. Journal of Biomechanics, 30(10), 1051–1058.

75. Neptune, R. R., Kautz, S. A., & Zajac, F. E. (2000). Muscle contributions to specific biomechanical functions do not change in forward versus backward pedaling. Journal of biomechanics, 33(2), 155-164.

76. Nordeen-Snyder KS. The effect of bicycle seat height variation upon  oxygen  consumption and  lower  limb  kinematics.  Med Sci Sports Exerc 1977; 9: 113-7

77. Origenes MM , Blank SE, Schoene RB (1993) May;25(5):608-12.Exercise ventilatory response to upright and aero-posture cycling. Med Sci Sports Exerc

78. Price D, Donne B (1997) Effect of variation in seat tube angle at different seat heights on submaximal cycling performance in man.. J Sports Sci. Aug;15(4):395-402

79. Raasch, C. C., & Zajac, F. E. (1999). Locomotor strategy for pedaling: Muscle groups and biomechanical functions. Journal of Neurophysiology, 82, 515–525.

80. Raymond CH, Joseh KF Gabriel YF (2005) Muscle recruitment pattern in cycling: a review. Physical therapy in sport 6: 89-96.

81. Reiser R. & Peterson M. L. (1998). Lower-extremity output in recumbent cycling: a literature review. Human Power 45: 6–13.

82. Roul Reiser and M. L. Peterson

83. Riley, P. O., Franz, J., Dicharry, J., & Kerrigan, D. C. (2010). Changes in hip joint muscle–tendon lengths with mode of locomotion. Gait & Posture, 31(2), 279-283.

84. Saibene, F., & Minetti, A. E. (2003). Biomechanical and physiological aspects of legged locomotion in humans. European Journal of Applied Physiology, 88(4-5), 297-316.

85. Sanderson, D. J., Martin, P.E., Honeyman, G., Keefer, J. (2006). Gastrocnemius and soleus muscle length, velocity, and EMG. Journal of Electromyography and Kinesiology 16 642–649.

86. Schmidt-Nielsen K. Locomotion: energy cost of swimming, flying, and running. Science. 1972: 177: 222-228.

87. Seeley, M. K., Umberger, B. R., Clasey, J. L., & Shapiro, R. (2010). The relation between mild leg-length inequality and able-bodied gait asymmetry. Journal of Sports Science & Medicine, 9(4), 572.

88. Seminati, E., Nardello, F., Zamparo, P., Ardigò, L. P., Faccioli, N., & Minetti, A. E. (2013). Anatomically Asymmetrical Runners Move More Asymmetrically at the Same Metabolic Cost. PloS one, 8(9), e74134.

89. Shennum PL, Devries HA. The effect of saddle height on oxygen consumption during ergometer work. Med Sci Sports 1976; 8: 119-21

90. Silder A, Gleason K, Thelen DG (2011) Influence of bicycle seat tube angle and hand position on lower extremity kinematics and neuromuscular control: implications for triathlon running performance.. J Appl Biomech. Nov;27(4):297-305.

91. Smak, W., Neptune, R. R., & Hull, M. L. (1999). The influence of pedaling rate on bilateral asymmetry in cycling. *Journal of biomechanics*, 32(9), 899-906.

92. Steele, K. M., Seth, A., Hicks, J. L., Schwartz, M. S., & Delp, S. L. (2010). Muscle contributions to support and progression during single-limb stance in crouch gait. Journal of biomechanics, 43(11), 2099-2105.

93. Steele, K. M., Seth, A., Hicks, J. L., Schwartz, M. H., & Delp, S. L. (2013). Muscle contributions to vertical and fore-aft accelerations are altered in subjects with crouch gait. Gait & posture, 38(1), 86-91.

94. Thelen, D. G., Chumanov, E. S., Hoerth, D. M., Best, T. M., Swanson, S. C., Li, L., &Heiderscheit, B. C. (2005). Hamstring muscle kinematics during treadmill sprinting. Medicine & Science in Sports & Exercise, 37(1), 108-114.

95. Terkelsen, K. E., Clark, A. L., & Hillis, W. S. (1999). Ventilatory response to erect and supine exercise. Medicine & Science in Sports & Exercise, 31(10), 1429-1432.

96. Tokui, M., & Hirakoba, K. (2008). Estimation of oxygen cost of internal power during cycling exercise with changing pedal rate. Journal of Physiological Anthropology, 27(3), 133-138.

97. Too, D. (1990). Biomechanics of cycling and factors affecting performance. Sports Medicine, 10(5), 286-302.

98. Too D, Landwer GE 2000 the effect of pedal crank arm length on joint angle and power production in uprigth cycle ergometry J sport Scie 18:153-161

99. Willems P.A., Cavagna G.A., Heglund N.C. (1995) External, internal and total work in human locomotion. J. Exp. Biol. 198: 379-393.

100. Winter, D. A. (1979). A new definition of mechanical work done in human movement. Journal of Applied Physiology, 46(1), 79-83.

101. Wilson, D. G., Forrestall, R., & Hendon, D. (1984). Evolution of recumbent bicycles and the design of the avatar bluebell. Proceedings of the Second International Human Powered Vehicle Scientific Symposium, 92-103. Long Beach, CA:IHPVA, Box 2068, Seal Beach, CA.

102. Whittle M.W. (1997) Three-dimensional motion of centre of gravity of the body during walking. Hum. Mov.Sci. 16: 347-355.

103. Xiao, M., & Higginson, J. (2010). Sensitivity of estimated muscle force in forward simulation of normal walking. Journal of applied biomechanics, 26(2), 142.

104. Xiao, M., & Higginson, J. (2007). Simulation study of walking patterns with knee osteoarthritis using opensim. In American Society of Biomechanics Annual Meeting.

105. Zajac, F. E. (1988). Muscle and tendon: properties, models, scaling, and application to biomechanics and motor control. Critical Reviews in Biomedical Engineering, 17(4), 359-411.

106. Paola Zamparo, Alberto E. Minetti, Pietro E. di Prampero (2002). Mechanical efficiency of cycling with a new developed pedal–crank. Journal of Biomechanics 35 1387–1398

107. Zarrugh MY, Radcliffe CW. (1978). Predicting metabolic cost of level walking. Eur J Appl Physiol Occup Physiol.: 38: 215-223.

108. Zarrugh MY, Todd FN, Ralston HJ. (1974). Optimization of energy expenditure during level walking. Eur J Appl Physiol Occup Physiol.: 33: 293-306.

# Ringraziamenti